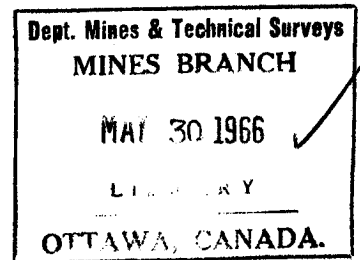




CANADA

PILLAR LOADING

Part III: Field Measurements



D. F. COATES

FUELS AND MINING PRACTICE DIVISION

DEPARTMENT OF MINES AND
TECHNICAL SURVEYS, OTTAWA

MINES BRANCH

RESEARCH REPORT

R 180

*R181 not published

Price \$1.25

FEBRUARY 1966

© Crown Copyrights reserved

Available by mail from the Queen's Printer, Ottawa,
and at the following Canadian Government bookshops:

OTTAWA

Daly Building, Corner Mackenzie and Rideau

TORONTO

Mackenzie Building, 36 Adelaide St. East

MONTREAL

Aeterna-Vie Building, 1182 St. Catherine St. West

or through your bookseller

A deposit copy of this publication is also available
for reference in public libraries across Canada

Price \$1.25

Catalogue No. M38 -1/180

Price subject to change without notice

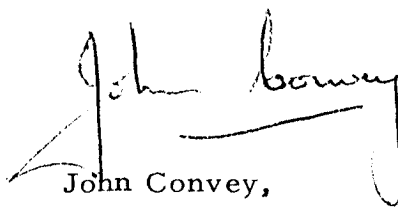
ROGER DUHAMEL, F.R.S.C.
Queen's Printer and Controller of Stationery
Ottawa, Canada

1966

FOREWORD

It is Mines Branch policy to promote research, to support universities and to disseminate information on subjects of importance to the mineral industry. With the traditional strength, among other subjects, of McGill University in applied mechanics, it has been natural for its Department of Mining Engineering and Applied Geophysics to display a leading interest in the development of the new subject of rock mechanics and in the training of postgraduate students in this subject. The co-operative effort of our two organizations has produced in a doctoral thesis, on which this report is based, what seems to be a significant contribution to the science of mining.

Dean D. L. Mordell and Professor R. G. K. Morrison, Chairman of the Department of Mining Engineering and Applied Geophysics, are to be commended for promoting this work. The Mines Branch is glad to publish this work, in a series of three reports of which this is the third, so that it can receive wide distribution amongst those interested in a basic study of an important element of mine structures -- the pillar.

A handwritten signature in cursive script that reads "John Convey". The signature is written in dark ink and is positioned above the printed name and title.

John Convey,
Director,
Mines Branch.

Mines Branch Research Report R 180

PILLAR LOADING. Part III. Field Measurements

by

D. F. Coates^x

- - -

ABSTRACT

This work is in the area of engineering theory. It is concerned with the combining of existing scientific theories into a rational hypothesis for predicting the loading of pillars. Hitherto, this has only been possible in a very crude way and only for horizontal workings.

Analytical work to predict pillar loadings for long mining zones in elastic ground results in equations which include, in the form of dimensionless parameters, the significant geometrical and material properties affecting pillar loading. Measurements of pillar stresses in laboratory models of gelatin, of Araldite-type materials, of mortar, and of steel show that it is possible to predict the variation of pillar loading--with location within the mining zone--with variation of pillar height--with variation in pillar breadth--with the number of pillars across the mining zone--with the variation of the compressibility of the pillar ground with respect to that of the walls--with variation in the magnitude of the field stress component acting transversely to the mining zone or vein--and, above all, with the extraction ratio.

The results of pillar stress measurements in a lead mine, two iron mines, a coal mine and a uranium mine indicate that the most significant parameter causing deviation from the predicted pillar stresses is the variation in the relative compressibility of the pillar rock.

The tributary area theory was found not to predict actual pillar loadings with an acceptable accuracy nor to account for changes in pillar loadings resulting from changes in the above factors included in the new hypothesis.

^xHead, Mining Research Laboratories, Fuels and Mining Practice Division,
Mines Branch, Department of Mines and Technical Surveys, Ottawa, Canada.

Direction des mines

Rapport de recherches R 180

LA CHARGE DES PILIERS. PARTIE III:
MESURES SUR LES LIEUX

par

D. F. Coates*

- - - -

RÉSUMÉ

Le présent travail de recherche sur la charge des piliers se range dans ce que l'on pourrait appeler le domaine du génie théorique. Il cherche à combiner les théories scientifiques existantes pour en arriver à une hypothèse rationnelle sur la prédiction de la charge des piliers. Jusqu'ici, cela n'a été possible que d'une façon très rudimentaire et seulement dans le cas où l'extraction se faisait à l'horizontale.

Les travaux analytiques effectués en vue de prédire le régime de charge des piliers en zones d'extraction étendues, en terrain élastique, permettent d'obtenir des équations qui, sous forme de paramètres sans dimensions, renferment les propriétés géométriques et physiques déterminantes qui influent sur le régime de charge des piliers. Les mesures de contraintes de piliers, dans des modèles de laboratoire en gélatine, en matériaux de type araldite, en mortier et en acier ont montré qu'il était possible de prédire les changements du régime de charge des piliers selon leur emplacement à l'intérieur de la zone d'exploitation, leur hauteur, leur largeur, leur nombre à travers la zone d'exploitation, la compressibilité de la roche du pilier par rapport à celle des parois, l'intensité de la composante de la contrainte du terrain agissant transversalement au filon ou à la zone d'exploitation et surtout selon le rythme d'extraction.

Les résultats obtenus à la suite de mesures de contraintes dans les piliers d'une exploitation de plomb, d'uranium, d'un charbonnage et de deux mines de fer démontrent que le paramètre le plus important et responsable

*Chef, Laboratoires de recherche en génie minier, Division des combustibles et du génie minier, Direction des mines, ministère des Mines et des Relevés techniques, Ottawa, Canada.

d'un écart dans la prédiction des contraintes du pilier, réside dans une variation de la compressibilité de la roche du pilier.

Il a été établi que la théorie de la zone tributaire n'a pu ni prédire avec un certain degré d'exactitude les charges actuelles du pilier ni expliquer les variations dans le régime de charge des piliers résultant de changements dans les facteurs susmentionnés de la nouvelle hypothèse.

=

CONTENTS

	<u>Page</u>
Foreword	i
Abstract	ii
Résumé	iii
Introduction	1
Field Measurements	4
Lead Mine	4
Geology. Mining. Method of Measurement. Experimental Results. Analysis of Data.	
Iron Mine A	12
Geology. Mining. Experimental Results. Analysis of Data.	
Coal Mine	17
Geometry. Method of Measurement. Experimental Results. Analysis of Data.	
Iron Mine B	21
General Geology. Stratigraphy. Structural Geology. Mining. Method of Measurement. Experimental Results. Analysis of Data.	
Uranium Mine	37
General Geology. Structural Geology. Lithology. Mining. Method of Measurement. Experimental Results. Analysis of Data.	
Conclusions	61
Acknowledgements	62
Bibliography	63
Appendix: Glossary of Abbreviations	64
Conversion Tables	71

FIGURES

<u>No.</u>		<u>Page</u>
1.	Ideal mining zones: (a) horizontal orebody (b) vertical orebody	2
2.	Plan of lead mine (Ref. 4)	5
3.	Comparison of actual pillar loadings with the tributary area theory (TA) and the new hypothesis (HYP)	10
4.	Plan of iron mine A (Ref. 4)	13
5.	Sections of iron mine A (Ref. 4)	14
6.	Plan of a coal mine	18
7.	Location of field stress holes in iron mine B	24
8.	Plan and sections, Pillar 42	27
9.	Geological section of mine through Pillar 42	28
10.	Geological section of Pillar 42	29
11.	Geological plan of Pillar 42, 2-2 Sublevel	30
12.	Geological plan of Pillar 42, 2-1 Sublevel	31
13.	Pillar 51, plan and sections	33
14.	Geological section through Pillar 51	34
15.	Geological plans of Pillar 51	35
16.	Regional geology of uranium mine area	38
17.	Vertical geological section through uranium mine	39
18.	Plan of uranium mine	41
19.	Plan of stope 9 W 9 (Ref. 12)	44
20.	Plan of stope 1009 (Ref. 12)	45
21.	Plan of stope 1109 (Ref. 12)	46
22.	Section of west rib pillar, 9 W 9 stope (Ref. 12)	48
23.	Section of centre pillar, 9 W 9 stope (Ref. 12)	49
24.	Section of east rib pillar, 9 W 9 stope (Ref. 12)	50

FIGURES (Concluded)

<u>No.</u>		<u>Page</u>
25.	Section of west rib pillar, 1009 stope (Ref. 12)	51
26.	Section of central pillar, 1009 stope (Ref. 12)	52
27.	Section of east rib pillar, 1009 stope (Ref. 12)	53
28.	Section of west rib pillar, 1109 stope (Ref. 12)	54
29.	Section of centre pillar, 1109 stope (Ref. 12)	55
30.	Section of east rib pillar, 1109 stope (Ref. 12)	56

TABLES

1.	Experimental Data from Lead Mine	7
2.	Analysis of Data from Lead Mine	9
3.	Change in Parameters Required to Explain Deviation of Measured from Hypothesis in Lead Mine	11
4.	Experimental Data from Iron Mine A	15
5.	Analysis of Data from Iron Mine A	17
6.	Experimental Data from Coal Mine	20
7.	Analysis of Data from Coal Mine	20
8.	Experimental Data from Iron Mine B	26
9.	Analysis of Data from Iron Mine B	36
10.	Experimental Data from Uranium Mine	43
11.	First Analysis of Data from Uranium Mine	58
12.	Second Analysis of Data from Uranium Mine	60

INTRODUCTION

A new hypothesis has been developed for the determination of pillar loads that includes more of the significant factors than are contained in the older tributary area theory (1)^x. The hypothesis is based on the relation between the stress in a pillar and its deflection; the deflections of the walls at the pillar are, of necessity, equal to those of the pillars. By analysing the various components of the deflections that occur in the walls as a result of mining, the resultant stresses in the pillars can be predicted.

The hypothesis represents the cases where the mining zone is very long in the direction perpendicular to the span. Because the origin is placed at mid-span and mid-height, use is made of the semi-span, l , the semi-height of the pillar, h , and the distance to the location of any pillar, x , as shown in Figure 1. The field stress (or pre-mining stress) normal to the vein is S_o , and the field stress in the direction transverse to the mining zone is S_t .

To test the validity of the hypothesis, the measurements obtained from various series of models have been compared with those that would have been predicted by the hypothesis. The models in some cases were made of gelatin; in other cases, the more conventional Araldite-type plastics were used, with the stresses determined photoelastically. Mortar was used in another series, and our own experiments were with steel plates and strain gauges (2).

The agreement between the results from the various model studies is very good. Furthermore, they confirm that the factors included in the hypothesis are significant with respect to pillar loading and that, in most cases, the older theory cannot be relied on for computing pillar stresses. The model tests also indicate that the hypothesis itself does not include all the significant mechanisms; consequently, it has been modified empirically to provide a better fit to the experimental data. The equations developed from the theoretical and model work are as follows:

^x These numbers refer to the sources of information listed in the Bibliography at the end of this report.

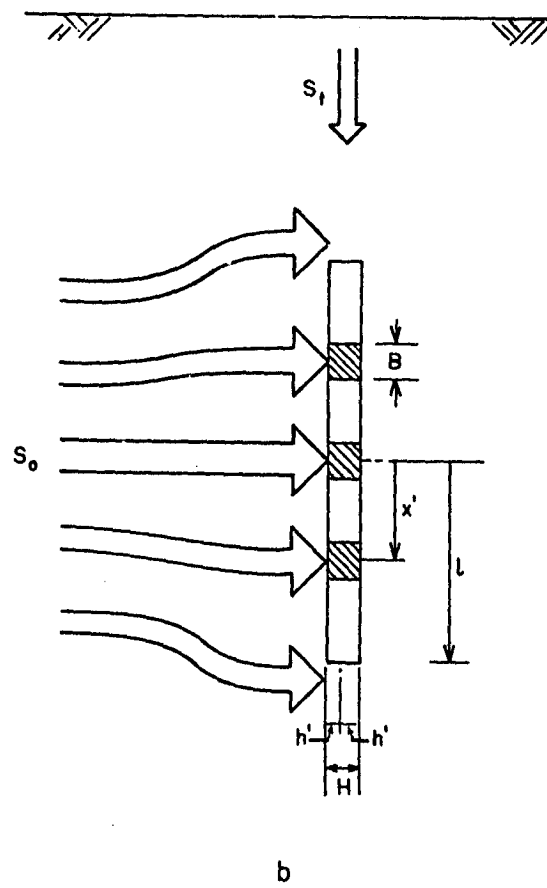
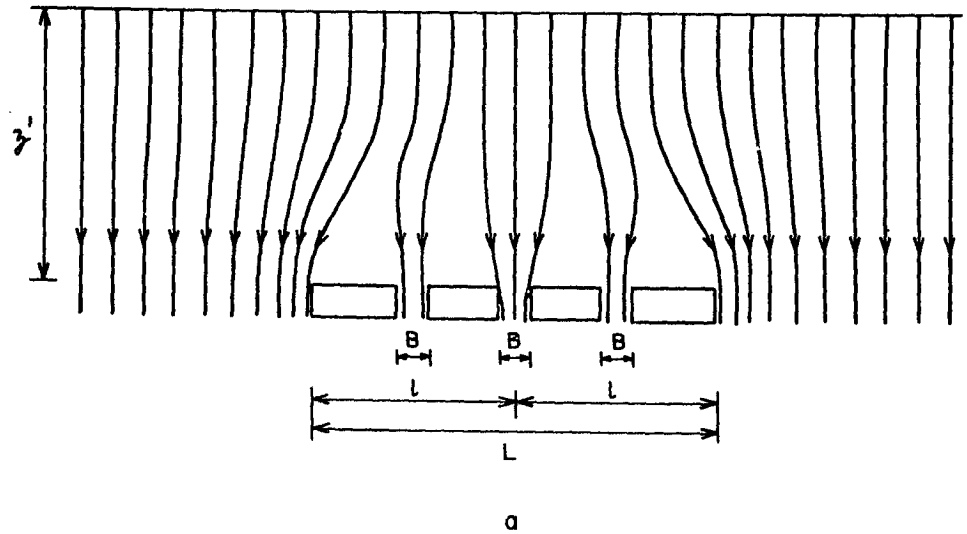


Figure 1. Ideal mining zones: (a) Horizontal orebody
(b) vertical orebody.

$$\therefore \frac{\Delta \sigma_P}{S_o} = \frac{2R(1-x/5+h) - kh(1-w+w_p n)}{hn + 1.8(1-R)(1+1/N)(1+h/(1-x/5)) + 2Rb(1-w)/\pi} \quad \text{Eq. 1}$$

$$\frac{\Delta \sigma_P}{S_o} = \frac{2R(1-x/5+2h) + RK_b' - kh(1-w+2w_p n)}{2hn + (1.8(1+h/(1-x/5)) + (2K_b'/3)(1+h/(1-x^2)))(1-R)(1+1/N) + 4bR(1-w)/\pi} \quad \text{Eq. 2}$$

where $\Delta \sigma_P$ is the increase in pillar stress resulting from mining out the adjacent stopes;

S_o is the normal field stress perpendicular to the vein;

R is the extraction ratio;

$x = x'/l$, the dimensionless x-coordinate of the particular pillar;

$h = h'/l$, the dimensionless height of the pillar;

$k = S_t/S_o$, the ratio of transverse to normal field stress components;

$w = \mu/(1-\mu)$, and μ is Poisson's ratio of the wall rock;

w_p is the same parameter for the pillar rock;

$n = M/M_p$ and $M = E/(1-\mu^2)$, with E being the modulus of deformation of the wall rock and M_p being the same parameter for the pillar rock;

r is the local extraction ratio based on the area tributary to the pillar in question;

b is equal to B/L , the dimensionless pillar width;

K_b' is a parameter that varies with the ratio of the depth below ground surface to the span of the mining zone for horizontal workings and equal to

$$(1-x^2)/(2z^3) + 1.2(1+w)(1-x^2)/z + (13-2w(1-x^2))/z^2 + 1 - 8/z^2 - 3w) z/32 + 0.884 F (1-x^2)/z^2;$$

$$F = 1 - 1/(2.26/z + 1);$$

and $z = z'/l$, with z' being the depth from the ground surface to the plane of the orebody.

FIELD MEASUREMENTS

Lead Mine

Geology. A typical stratigraphic succession at the Lead Mine starting at the ground surface is as follows: 20 ft of soil, 30 ft of mica schist and quartzite schist, 60 ft of mylonite, 15 ft of shale, 110 ft of various strata of sandstone at the bottom of which the ore occurs, 15 ft of arkos underlying the ore, and all overlying a granite basement (4).

The sandstones and the schists above the mylonite are of Cambrian age. The mylonite originated during the Caledonian upheaval, when the schists were pushed over the sandstones in a southeasterly direction. The base of the schists represents the thrust plane. The joints exposed on the roof and floor of the mine intersect the direction of the overthrust at approximately 45° .

The sandstone ore is about 30 ft thick. The formation is generally strong; however, layers of clay varying from a few millimetres to several centimetres in thickness occur. The individual strata of sandstone vary in thickness from about 1 ft to 10 ft.

In the mine area there are two main directions of jointing, which are roughly perpendicular to one another. Many of the joints contain gouge. The more predominant of the two systems runs in a north-south direction and is often water-bearing. The attitude of the joints is generally vertical.

Mining. The mining has been by a room-and-pillar method with the pillars conforming only roughly to a geometrical pattern (see Figure 2). Where the metal values were too low to provide good ore, larger pillars have been left than those simply required for roof support. In general the pillars are spaced 60 ft to 70 ft c c, with the free span of the roof varying from 45 ft to 60 ft. The pillar dimensions vary from 20 ft to 30 ft in breadth and are approximately square and generally 24 ft to 28 ft high. The extraction ratio, R, is about 90 per cent. The depth from the ground surface to the roof level is about 285 ft.

Method of Measurement. The method of measuring the in situ stresses included overcoring a small hole with a large coring bit and measuring the change in pressure on a gauge installed in the small hole. The small hole had a diameter of 26 mm and was drilled in increments of length of from 50 cm to 100 cm. The diameter of the overcoring was 87 mm. The overcoring is continued beyond the pressure gauge until the readings indicate that the stresses in the core have been completely relieved (4).

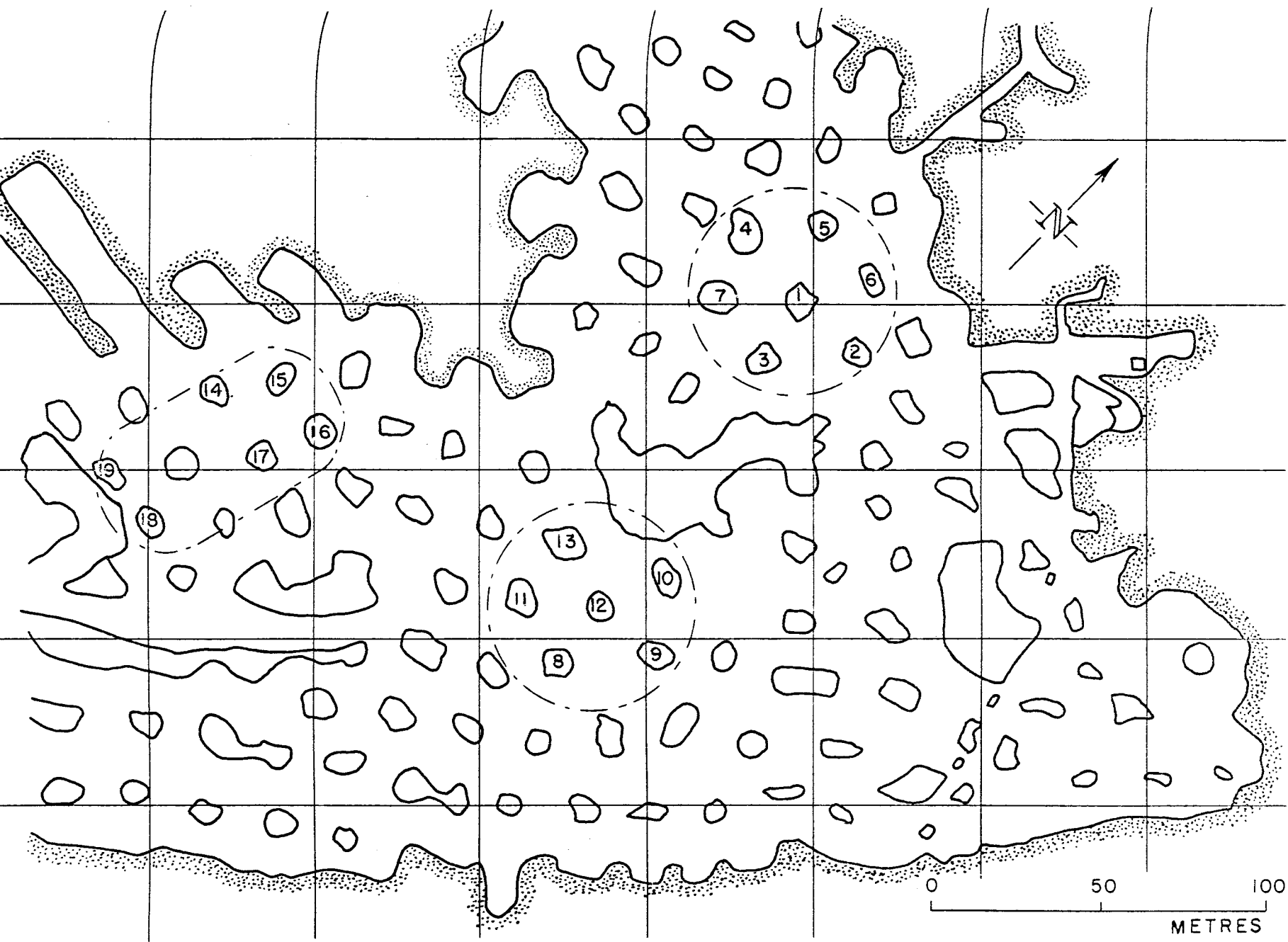


Figure 2. Plan of lead mine (Ref. 4).

The gauge itself is composed of three principal parts arranged transversely across the hole: a pressure cell, a set of wedges, and a bearing. The pressure cell consists of a nickel alloy spool serving as a core for a copper coil which is covered with a tube of Permalloy. It operates on the principle of magnetostriction.

After the gauge is installed in the drill hole and oriented in the desired direction, the cell is prestressed by a crank outside the drill hole which is used to set the wedges located between the pressure cell and the bearing. The degree of prestressing can be governed to some extent by this wedging action.

It is generally necessary to overcore about 5 cm beyond the cell to completely relieve the core of its stresses. Then, as the pressure cell measures the change in stress in only one direction, it is necessary to rotate the cell, usually 60° to the right, and advance it to a point in the small hole that is still subjected to the rock stresses. The overcoring is then repeated. The cell is advanced and reset into a third position, usually 60° to the left, and the operation again repeated. The distance between two consecutive positions of the cell is a minimum of 10 cm. However, for purposes of calculating the stress ellipse the three readings are assumed to be applicable to one point in the rock (4).

The cell is calibrated in the laboratory by using a block of material with a modulus of elasticity of the same order of magnitude as that of the rock. A hole is drilled in the block, which is then subjected to compression, the cell reading being plotted against the pressure on the block. This procedure is not necessarily foolproof, as the actual rock in the formation might be non-linear, anisotropic and have a relaxation modulus different from that of the loading modulus. In addition, the prestressing in the field, which is in excess of the maximum anticipated stress, can produce indentation in the walls of the drill hole. This action can be accounted for to some extent by the theory of elastic bearing; however, empirical substantiation of this theory in rock is still required. Some of these difficulties are overcome by testing the modulus of deformation at the location of the reading in the large-sized core that is obtained from overcoring.

Experimental Results. The results of the measurements of pillar stresses in this mine are shown in Table 1. The extraction ratio, R , is an average figure applicable to the entire mine. The height of the pillars, H , is also an average figure. Poisson's ratios, μ and μ_p , for both the wall rocks and the pillars were obtained from tests on the rock substance. These tests also indicated that the moduli of deformation of the wall rocks and pillar rocks were substantially the same (4).

TABLE 1

Experimental Data from Lead Mine (4)

$R = 0.9$, $H = 26$ ft, $z = 285$ ft, $k = 5$, $\mu = 0.25$, $n = 1$, $i = 0$

No.	N	L ft	B ft	B _o ft	x	$\Delta\sigma'_p$
L-1	4	375	24	47	0.24	2.2
L-2	4	375	23	43	0.48	6.6
L-3	4	375	28	52	0.10	6.5
L-4	4	375	33	30	0.03	3.8
L-5	4	375	25	43	0.35	4.1
L-6	4	375	21	45	0.58	0.6
L-7	4	375	30	43	0.11	6.8
L-8	6	520	24	45	0.25	7.0
L-9	6	520	25	39	0.12	5.9
L-10	6	520	27	26	0.04	4.0
L-11	6	520	30	44	0.10	4.0
L-12	6	520	21	39	0.09	7.2
L-13	6	520	31	42	0.38	3.4
L-14	7	530	21	42	0.62	1.8
L-15	7	530	23	36	0.65	2.3
L-16	7	530	23	29	0.55	5.5
L-17	7	530	23	38	0.35	5.2
L-18	7	530	25	23	0.56	4.6
L-19	7	530	23	26	0.21	6.0

The ratio of tangential to normal field stresses, k , or S_t/S_o , was obtained from measurements in the roof and floor. These measurements indicated that, at a depth into the rock of 1.3 m, the maximum horizontal stress was 150 ksc in a north-south direction, with the minimum horizontal stress being 100 ksc in the east-west direction. From the trend of measurements in individual holes it was seen that the surface rock had been damaged and partially relieved of stress for a depth of at least 0.8 m. From these stresses it was calculated that the transverse stress over both spans of the L-shaped mining area, which were both at 45° to the north-south direction, would be 125 ksc. Then by using the equation for the boundary stresses around an elliptical opening in an infinite solid (5) and assuming the 125 ksc is substantially a boundary stress, the ratio, k , is calculated to be equal to about 5.

The spans of the mining zones, L , are taken from the mine plan as shown in Figure 2, exercising some judgment on where the effective abutment line would start. The widths of the pillars, B , have been determined by taking the area of the pillar cross-section at the elevation at which the stress measurements were made and assuming a square shape.

The measurements of the increase in pillar stress, $\Delta\sigma_p'$, are the averages of several readings in each pillar.

Analysis of Data. Table 2 shows the results of the analysis of the data from the mine. The increase in stress predicted by the tributary area theory varies between 7.50 and 7.87. The increase in stresses for the individual pillars predicted by the hypothesis, using the general extraction ratio, R , of 90 per cent and modified as included in Equation 1 (which must be used when the general extraction ratio is given) as shown in the last column of Table 2, varies between 4.49 and 5.48.

All of the measurements of the increase in pillar stresses are much less than predicted by the tributary area theory. Some are less and some greater than predicted by the modified hypothesis, as shown in Figure 3. The most probable explanation for this deviation of the measured results from the prediction of the modified hypothesis is that many of the pillars had greater actual compressibility than the wall rocks. This would result in these pillars having less stress than predicted, and the adjacent pillars subjected to an increase in effective extraction ratio would have greater stress than predicted.

In Table 3 the changes in the parameters n and R required to give approximate agreement between the measured and the predicted increase in pillar stresses are shown. In the cases where the pillar stresses were less than predicted, the necessary changes in the parameter n , taking into account the variable damage that could occur to the pillar rock as a result of blasting, seem quite reasonable.

TABLE 2

Analysis of Data from Lead Mine

$R = 0.90$, $k = 5$, $\mu = 0.25$, n assumed 1, $i = 0$

No.	N	h	b	x	$\Delta \sigma'_p$	$\Delta \sigma'_p$	$\Delta \sigma'_p$
					MEAS	TA	HYP
L-1	5	0.068	0.064	0.24	2.2	7.50	4.81
L-2	5	0.068	0.057	0.48	6.6	7.50	4.57
L-3	5	0.068	0.071	0.10	6.5	7.50	4.94
L-4	5	0.068	0.082	0.03	3.8	7.50	4.98
L-5	5	0.068	0.062	0.35	4.1	7.50	4.72
L-6	5	0.068	0.053	0.58	0.6	7.50	4.49
L-7	5	0.068	0.076	0.11	6.8	7.50	4.92
L-8	6	0.053	0.093	0.25	6.9	7.72	5.28
L-9	6	0.053	0.094	0.12	6.9	7.72	5.45
L-10	6	0.053	0.106	0.04	4.0	7.72	5.56
L-11	6	0.053	0.117	0.10	4.0	7.72	5.42
L-12	6	0.053	0.082	0.09	7.2	7.72	5.55
L-13	6	0.053	0.121	0.37	3.4	7.72	5.05
L-14	7	0.053	0.082	0.62	1.8	7.87	4.89
L-15	7	0.053	0.094	0.65	2.3	7.87	4.79
L-16	7	0.053	0.092	0.55	5.5	7.87	4.87
L-17	7	0.053	0.090	0.35	5.2	7.87	5.13
L-18	7	0.053	0.100	0.06	4.6	7.87	5.48
L-19	7	0.053	0.090	0.21	6.0	7.87	5.31

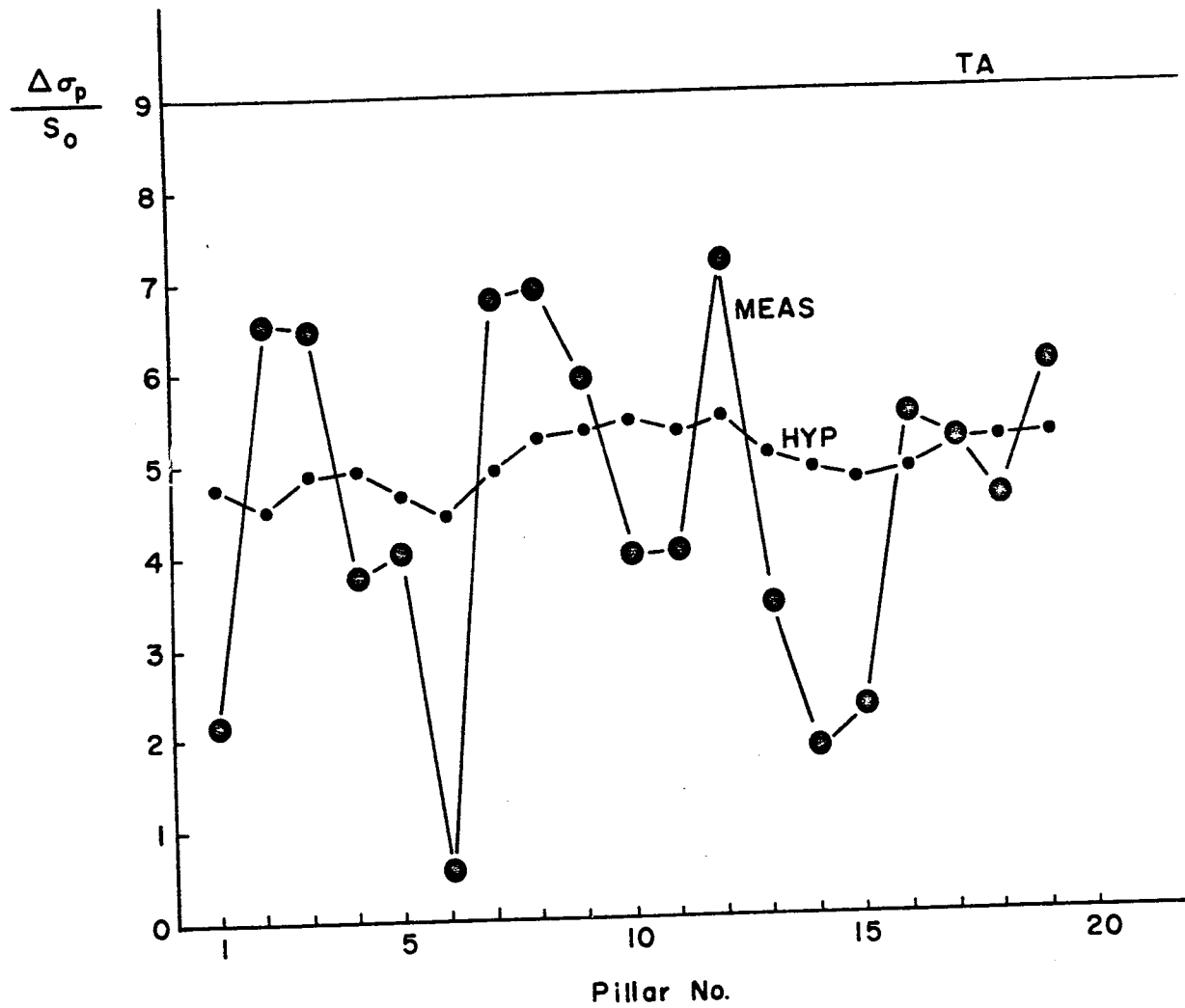


Figure 3. Comparison of actual pillar loadings with the tributary area theory (TA) and the new hypothesis (HYP).

TABLE 3

Change in Parameters Required to Explain Deviation
of Measured from Hypothesis in Lead Mine

No.	Changed to	$\Delta\sigma'_p$	$\Delta\sigma'_p$
		MEAS	HYP
L-1	n = 4	2.2	2.1
L-2	R = 0.93	6.6	6.1
L-3	R = 0.93	6.5	6.6
L-4	n = 2	3.8	3.9
L-6	n = 10	0.6	0.6
L-7	R = 0.93	6.8	6.6
L-8	R = 0.93	6.9	7.2
L-10	n = 2	4.0	4.4
L-11	n = 2	4.0	4.3
L-12	R = 0.93	7.2	7.3
L-13	n = 3	3.4	3.4
L-14	n = 7	1.8	1.7
L-15	n = 5	2.3	2.3
L-18	n = 2	4.6	4.4

In the cases where the pillar stresses were greater than that predicted by the modified hypothesis, it is probable that the explanation lies in the fact that adjacent pillars had relaxed, e.g., at pillar 12 the adjacent pillars 10, 11 and 13 had relaxed so that they were not carrying their full share of the roof load with the consequence that the effective extraction ratio locally was more than the average value. It can be seen from Table 3 that only a slight change in the parameter, R, is necessary to change the predicted stresses.

It can also be seen by re-examining the experimental data that the minimum values of measured stresses were obtained on the smaller pillars. This might be expected as a result of the higher probability of smaller pillars having their average compressibility more adversely affected by the release of side constraint and also by the blasting operations.

In addition, there seems to be a rough correlation of pillar stresses with the location, or parameter x; the highest values tending to be found close to the centreline of the span and the lowest values towards the abutments.

Another reason for deviation of measured values from predicted values of pillar loading is, of course, the variations arising from the experimental technique, which cannot be considered perfect.

Iron Mine A

Geology. The ore deposit of Iron Mine A consists of magnetite. The lenses dip at 60° to 75°. The rock of the hangingwall and footwall is leptite and granite, with the latter containing bodies of pure quartz. At the surface of contact between the country rock and the ore at both walls, there are clay deposits. Few joints are found in these rocks (4).

The ore in the shaft pillar is of coarse texture and of rather low strength. Thick bands of granite or leptite occur in this ore parallel to the walls, thus acting as reinforcement.

Mining. The ore has been mined out from the ground surface down 60 m for a distance of 470 m on strike (see Figures 4 and 5). From 60 m down to 235 m, mining has been completed on the same length of strike but a shaft pillar 50 m in breadth was left (4).

Experimental Results. The method of measuring the in situ stresses in this mine was the same as used in the lead mine as described above (4). A series of measurements was conducted in the crosscut passing through the pillar. These measurements were made in the granite or leptite bands. Measurements were also made in the footwall drift. Table 4 contains the results of these measurements.

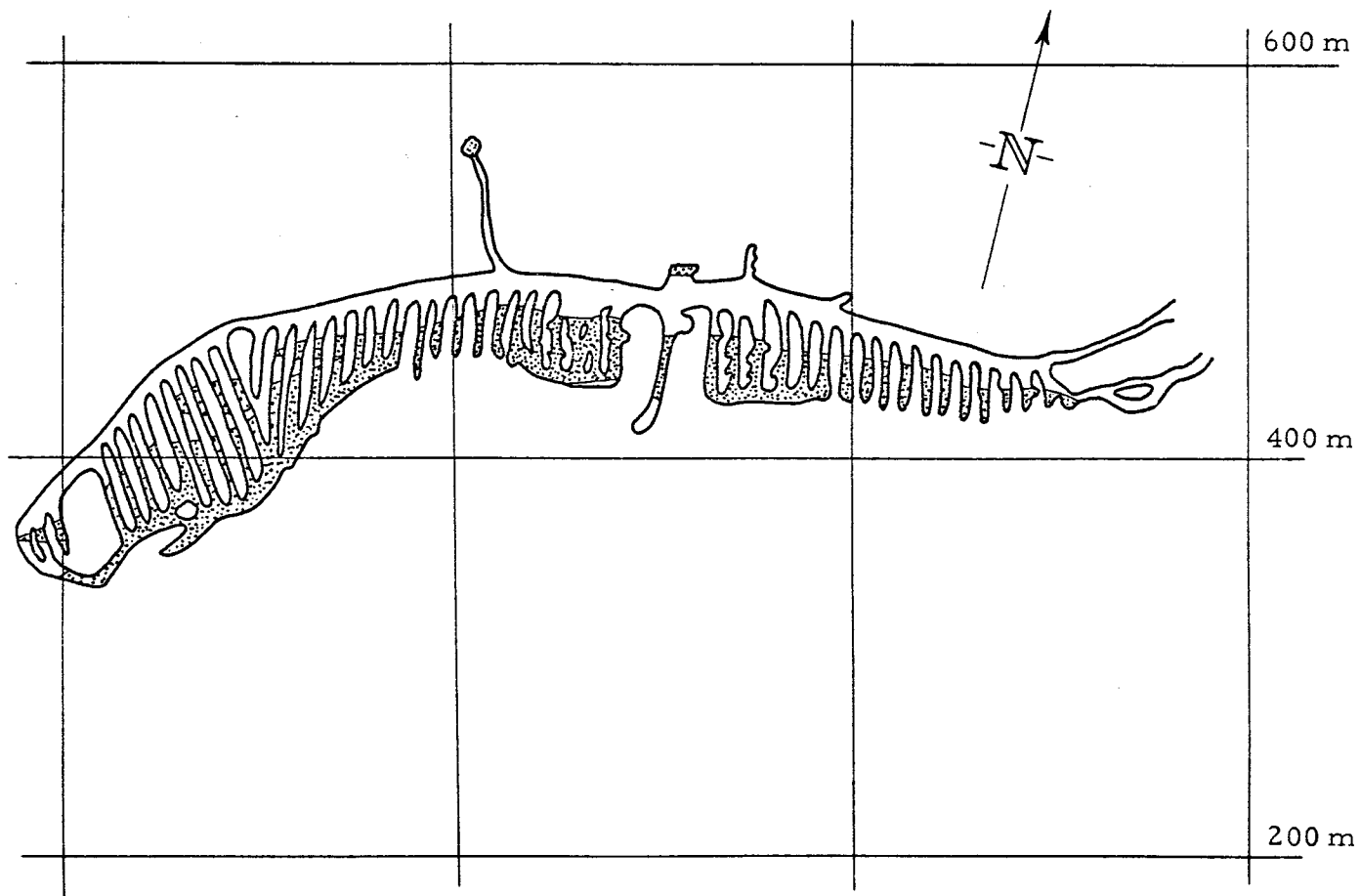
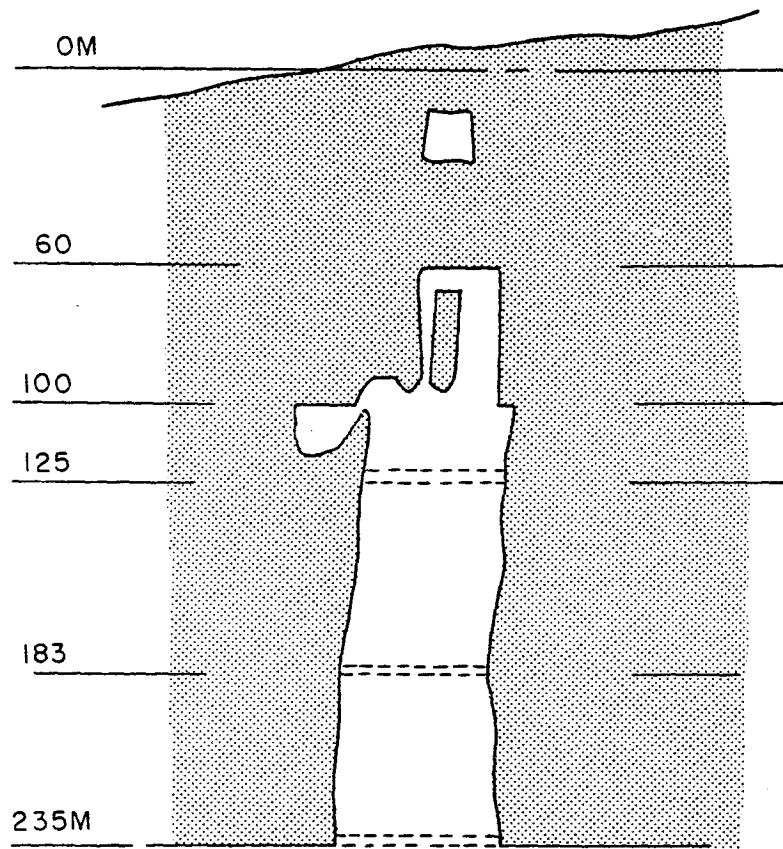
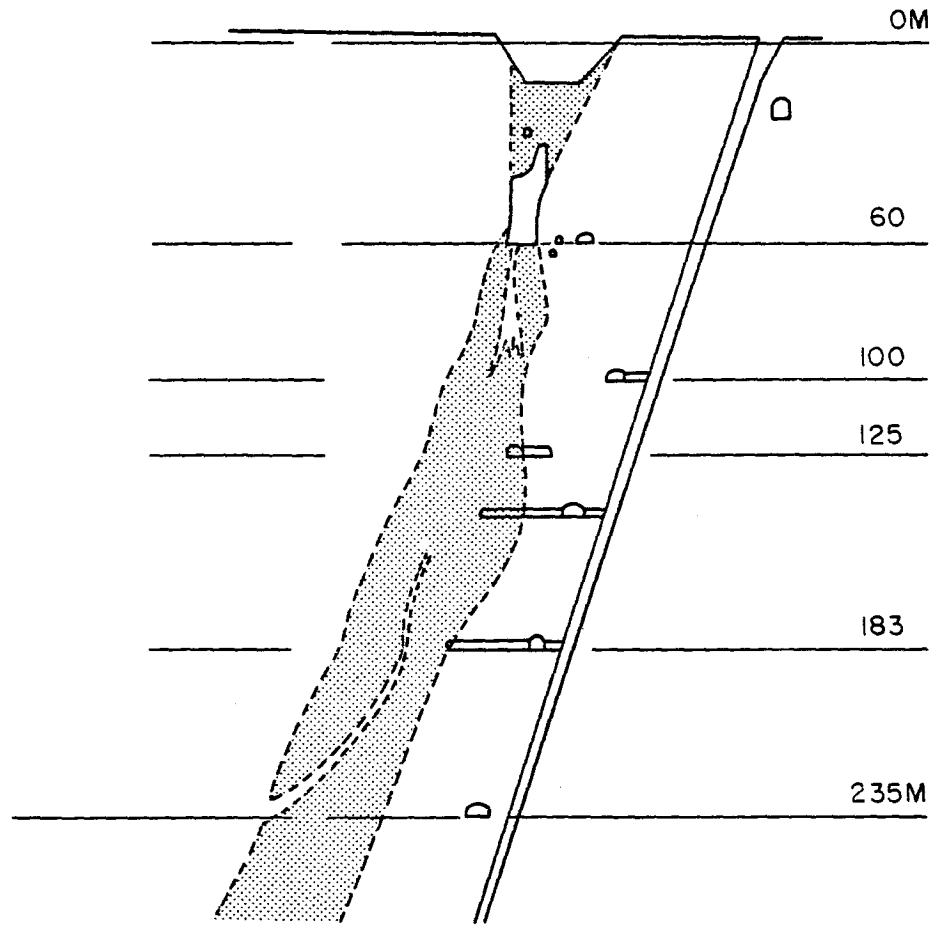


Figure 4. Plan of iron mine A (Ref. 4).



SECTION PARALLEL TO VEIN



VERTICAL SECTION PERPENDICULAR TO STRIKE

Figure 5. Sections of iron mine A (Ref. 4).

TABLE 4

Experimental Data from Iron Mine A (4)

N = 1, R = 0.895, L = 470m, H = 40m, B = 50m, x = 0.17, i = 67°

No.	z	^y S _v	S _o	S _t	σ _p
	m	ksc	ksc	ksc	ksc
M-1	100	135	-	-	250
M-3	100	-	-	220	-
M-4	123	225	-	-	450
M-6	123	130	-	-	460
M-11	183	240	-	-	510
M-15	125	-	-	250	-
M-16	150	-	-	200	-
M-18	232	-	-	-	570
M-19	232	260	-	-	450
M-21	290	-	^x 240	280	-
M-22	290	-	^x 110	360	-
M-23	290	200	-	360	-

^x Must be affected by diffraction of field stress under stopes.

^y Measured in or near pillar.

Analysis of Data. Table 4 also contains the measurements in the pillar of the vertical stress, S_v . In a uniform material with a steep dip, the vertical stress should be approximately equal to the vertical field stress and hence normally equal to the gravitational stress at that elevation. It can be seen that all measurements exceed the gravity stress; e.g., starting at point M-1 the gravity stress would be 25 ksc, and then at M-23 it would be 72.5 ksc.

Two mechanisms probably cause the measured values of vertical stress to exceed gravitational stresses. First, the concentration of the component of gravity stress normal to the vein in the pillar would tend to increase the vertical stress in the pillars; however, this effect should not be great. Second, with all the measurements being made in the competent bands of granite or leptite, it is almost certain that these bands would carry some of the weight of the adjacent incompetent ore similar to a structural sandwich of materials with different moduli of deformation.

The measurements, in the walls below the stoping area, of stresses normal to the walls, S_o , undoubtedly include the effects of the diffraction of the field stress under the stopes. These measuring points, M-21 and M-22, were at an elevation of approximately 50 metres below the bottom of the stopes and 50 metres back into the footwall from the plane of the vein. From the geometry of the mining opening, it can be determined that the stress concentration factor at such a point would be about 2. Consequently, the field stress, S_o , might be between 55 ksc and 120 ksc at the elevation of 50 metres below the bottom of the stope. There is no evidence on which to judge what this stress might be at higher elevations, other than the pillar stress measurements which are more or less uniform from a depth of 123 metres down to a depth of 232 metres.

The measurements of the horizontal stress parallel to the vein, S_t , might have included a minor concentration resulting from the diffraction of the stress field around the stopes. However, taking into account the long geometry of the stopes this factor would be almost insignificant and hence is ignored. There is some indication that this horizontal field stress might increase with depth. However, an average value for the full length of the pillar might be 250 ksc.

In determining the value of the modulus of deformation of the pillar in the direction normal to the walls, use was made of wall rock samples giving 7.7×10^6 psi. From the description of the pillar rock it was judged that the pillar modulus might be about 3×10^6 psi. Consequently, for purposes of computations, the ratio $n = 2.5$ has been used.

In Table 5 the results of the analysis of the measurements are shown. The increase in pillar loading, expressed as a ratio of the field stress normal to the vein, $\Delta\sigma_p'$, has been calculated assuming the

TABLE 5

Analysis of Data from Iron Mine A

$N = 1, R = 0.895, h = 0.085, b = 0.106, x = 0.17,$
 $k = 2.1-4.5, \mu = 0.2, n = 2.5, i = 67^\circ$

No.	$\Delta\sigma'_P$		$\Delta\sigma'_P$	$\Delta\sigma'_P$	
	MEAS			TA	HYP
	Min	Max		Min	Max
M-1	1.1	3.5	8.5	2.16	2.57
M-4	2.8	7.2	8.5	2.16	2.57
M-6	2.8	7.4	8.5	2.16	2.57
M-11	3.3	8.3	8.5	2.16	2.57
M-18	3.8	9.3	8.5	2.16	2.57
M-19	2.8	7.2	8.5	2.16	2.57

field stress to have a maximum value of 120 ksc and a minimum value of 55 ksc. Assuming the field stress parallel to the vein, S_t , has a constant value of 250 ksc, then the ratio k would have a value between 2.1 and 4.5, using the previous values for S_0 . With these two values of k , the minimum and maximum increases in pillar loading have been computed.

From the table, two points can be seen. First, the pillar stresses are considerably less than would be predicted by the tributary area theory, with the exception of the maximum value of M-18. Second, the minimum values of the other points are fairly close to those predicted by the modified hypothesis.

Coal Mine

Geometry. Tests were conducted in the centre of a large mined-out area (see Figure 6) approximately 480 ft below the ground surface. The pillars, nominally 50 ft square, were separated by bords, or rooms, 20 ft wide giving an extraction ratio of approximately 0.50. The coal seam was approximately 24 ft thick, of which 10 ft was being mined leaving 14 ft in the roof. The seam was approximately horizontal in the test area (6).

Laboratory compression tests were conducted on 10-in. diameter cores obtained from the overcoring procedure. The purpose of the tests was to determine the extent to which the core behaved as an elastic

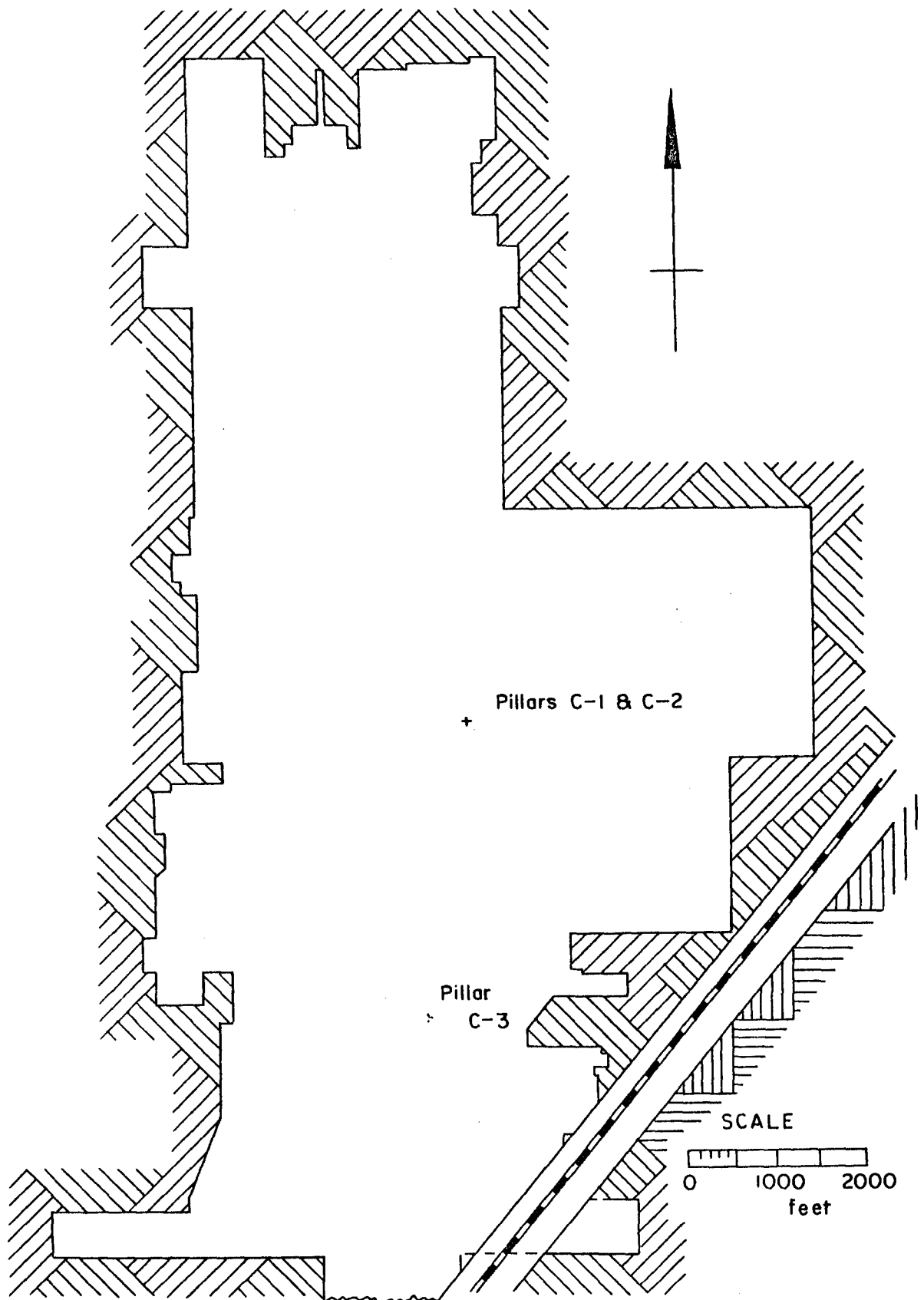


Figure 6. Plan of a coal mine.

material; the amount of residual strain, if any, on loading and unloading; the modulus of deformation; and Poisson's ratio of the coal. The test data indicated that, for the stress range in which the measurements were being made, it was reasonable to assume that the coal was behaving in an elastic manner. Also, on unloading the samples, the amount of residual strain was found to be negligible. The modulus of elasticity of the coal was 0.82×10^6 psi, and Poisson's ratio at 1000 psi was 0.28.

Method of Measurement. The method of measuring the in situ stress was by overcoring a small hole, $1\frac{1}{2}$ in. diameter, with a large coring bit, 10 in. in diameter. The small hole was drilled through the pillar so that a borehole deformation meter could be inserted and withdrawn from one side while the overcoring was being conducted from the other side. Measurements were started at about 1 ft from the rib face of the coal, and proceeded throughout the pillar with measurements being taken along the hole at a spacing of about 2 ft (6).

The changes in diameter of the borehole resulting from the release of stress were obtained with deformation meters containing linear variable differential transformers. Two transformers were incorporated in one instrument so that two orthogonal diameters could be measured simultaneously. These measured deformations were then used to calculate the stresses in the ground before being relieved by overcoring. Changes in diameter as small as 10^{-5} in. over a range of 0.01 in. can be measured with these deformation meters.

Experimental Results. Tests were conducted in three coal pillars with locations as shown in Figure 6. Several measurements were made throughout each pillar. The vertical normal stress in the undisturbed ground was assumed to be equal to $1.2z$ or 576 psi (6). Using this figure and determining the average increase in stress, the experimental results are given in Table 6.

Analysis of Data. The analysis of the data collected in this work is given in Table 7. Owing to the very small ratio of depth to semi-span, z/l , Equation 2 was used for the prediction of the increased pillar stresses.

The measured values of the average increase in pillar stress is greater in all three pillars than that predicted by the tributary area theory. The comparison with the values predicted by the hypothesis is more favourable. The major factor in the hypothesis influencing the calculated results is that it includes the shape of the deflection of the roof and floor, which makes it possible with small ratios of z/L for pillars to be loaded in the centre of a mining area with greater stress than that predicted by the tributary area theory.

TABLE 6

Experimental Data from Coal Mine (6)

R = 0.5, H = 10 ft, B = 50 ft, z = 480 ft, $\mu_p = 0.28$

No.	N	L ft	x	$\Delta\sigma'_p$
C-1	71	5000	0	1.2
C-2	71	5000	0	1.4
C-3	64	4500	0.07	2.2

TABLE 7

Analysis of Data from Coal Mine

R = 0.5, k assumed 0.2, μ assumed 0.5, n assumed 1, i = 0

No.	N	h	b	z/t	x	$\Delta\sigma'_p$	$\Delta\sigma'_p$	$\Delta\sigma'_p$
						MEAS	TA	HYP
C-1	71	0.002	0.01	0.19	0	1.2	0.99	1.47
C-2	71	0.002	0.01	0.19	0	1.4	0.99	1.47
C-3	64	0.0022	0.011	0.21	0.07	2.2	0.98	1.47

Iron Mine B

General Geology. The iron formation of Iron Mine B lies within a complex assemblage of Pre-Cambrian volcanic and sedimentary rocks. Most of the series consists of volcanic rocks varying in composition from basalt to rhyolite and in structure from flow to fragmental. Two principal horizons of sedimentary rocks—iron formation and assorted clastics—occupy stratigraphic positions within this volcanic pile. Both sedimentary horizons are structurally concordant for the most part, with the enclosing volcanics reflecting relatively brief sedimentary interludes in a dominantly volcanic process (7).

Iron formation appears to have been formed during a relatively quiet period when chemical activity prevailed. The clastic rocks appear to have been somewhat uplifted, with attendant erosion and sedimentation.

Intrusive into the volcanic-sedimentary rocks are stocks and larger masses of granite and granitic gneiss, sill- and dike-like masses of diorite, and numerous diabase dikes.

Stratigraphy. A principal stratigraphic feature is the location of the iron formation at or near the contact between the acid volcanics below and the basic volcanics above. The ore member within the iron formation, siderite, is the lowest member and is up to 300 ft thick.

The siderite ranges from light grey to pale buff in colour. It is variable in distribution and thickness, and of massive, uniform structure, although finely laminated in some locations. It contains variable siliceous impurities, which are present either as disseminated grains and patches of chert or as thick, persistent chert zones, as well as chloritic and micaceous impurities. Adjacent to diabase dikes some siderite has been partly converted to magnetite.

Structural Geology. The main structural features of the area are relatively simple. The volcanic-sedimentary sequence forms the south limb of an east-west trending syncline which plunges eastward at 40° - 60° and has been slightly overturned to the north. Thus, the rocks dip steeply southward in monoclinical succession and have their tops to the north.

This monoclinical structure dips south at 80° with displacements downdip producing average dips of 60° - 70° . The strike is a few degrees north of east. Due to this overturning, the geological footwall becomes the mining hangingwall.

The iron formation has been segmented by a group of north-westerly trending cross faults with relative movement of the north-east side to the north-west. Horizontal movements can be as much as 2 miles.

Low angle east-west striking thrust faults are also present. Other smaller fault groups also exist. The entire assemblage of the volcanic-sedimentary rocks has been rendered more or less schistose by strong shearing; the prevailing schistosity strikes north 65° east and dips steeply southward.

Metadiorite intrusions probably occurred during the late stages of folding, inasmuch as intrusions are found in faults related to folding. Diabase dikes are the youngest rocks and were placed after folding.

West of the mining area, a major fold occurs in the banded iron formation at the surface and plunges easterly at 50° - 60° . The ore zone terminates on the surface in this area but is much confused by intense brecciation and faulting. Underground mining and diamond drilling have proven that the ore rakes east in a similar attitude.

Folded thrusts with dips 15° - 30° south have displaced the ore zone relatively northward and up. This feature is largely due to folding. The actual contact between the ore and the stratigraphically upper wall rock is always a flat thrust fault.

The major fault types can be classified into five groups. Flat thrust faults dipping 15° - 30° south are sinuous in plan and have a general east-west strike. A steeper series of thrust faults strike north 60° east and dip 60° southeasterly to 60° northwesterly. They have left-handed movement and have thinned the ore zone because of their large displacements at small angles to the orebody. Transcurrent faults strike east to south 60° east and dip steeply south. Relative movement is right-handed and is mostly horizontal. This type of faulting commonly has a thick breccia, whereas all other fault types are tight. Transverse-type faults strike north 35° east across the orebody, dipping steeply in some cases to the east and in other cases to the west. They have left-handed movement with a maximum of 250 ft of horizontal displacement, and are sometimes discontinuous. A strong displacement on one wall may not be apparent on the other wall. Another group of faults strikes northwesterly and dips steeply in some cases south-west and in other cases north-east. Relative movement is left-handed. Most of the diabase dikes follow these faults or tension fractures on the same strike.

As can be observed from the above, a complicated fault pattern has developed, probably during the late stages of folding. Faulting is more intense in the upper levels of the mine than at depth. Faulting may be developed in one or more stratigraphic units and missing in an adjoining unit. A great difference in relative competency of stratigraphic units, with each reacting differently to stress, has been suggested as the logical explanation (7).

Mining. A system of transverse stopes and pillars is mined, using blast hole stoping. Stopes 60 ft-75 ft broad extend from hangingwall to footwall between an undercut elevation and a crown pillar. Their heights are 200 ft. Rib pillars are 75 ft-80 ft in breadth, and the crown pillars are 70 ft in breadth. The first pillar to be blasted is T-shaped and breaks into stopes on either side. The remaining pillars are inverted L-shaped and break into one adjacent stope. Rib pillars are commonly reduced to about 60 ft in breadth prior to the final blast.

Method of Measurement. The method of measuring the in situ stresses included overcoring a small hole (EX) with a large coring bit (6 in.) and measuring the change in diameter of the small hole. The principle of this technique is that when the ground around the small hole is released from the constraint of the stress field, the borehole will deform into a shape that is a function of the stress change in the ground around the hole or, in other words, the original stress field.

The deformation meter that is used to measure the change in diameter of the small hole consists essentially of a small cantilever beam held in a tube along the axis of the hole, with a plunger on the end of the beam in contact with one side of the hole. Any change in diameter of the hole changes the deflection of the cantilever beam, and the associated change in strain in the beam is measured with foil strain gauges (8).

This deformation meter measures the change in one diameter at a time. Consequently, after the deformation meter has been overcored it is necessary to move it along the hole, change the orientation and overcore again. With the measurement of the changes in three diameters at different orientations, generally 60° apart, it is then assumed that the distance between the successive readings is not significant. The maximum and minimum normal stresses in the plane perpendicular to the axis of the hole can then be determined (9).

Experimental Results. A site was selected for field stress measurements in a hangingwall drift on a level 1100 ft below the ground surface. The site was well away from the areas that had been mined out. The location of the holes are shown in Figure 7. These holes were over 1500 ft from the nearest stope (10).

Hole No. 1 was drilled nearly parallel to strike and into the hangingwall. It was found to be in siderite containing a large proportion of sulphides towards the end of the hole. A small thrust fault running parallel to the contact zone was identified just below the collar of the hole. Difficulties were experienced here in obtaining stable readings from the deformation meter. The experimentation and modifications that resulted from this hole produced reliable results for the subsequent holes.

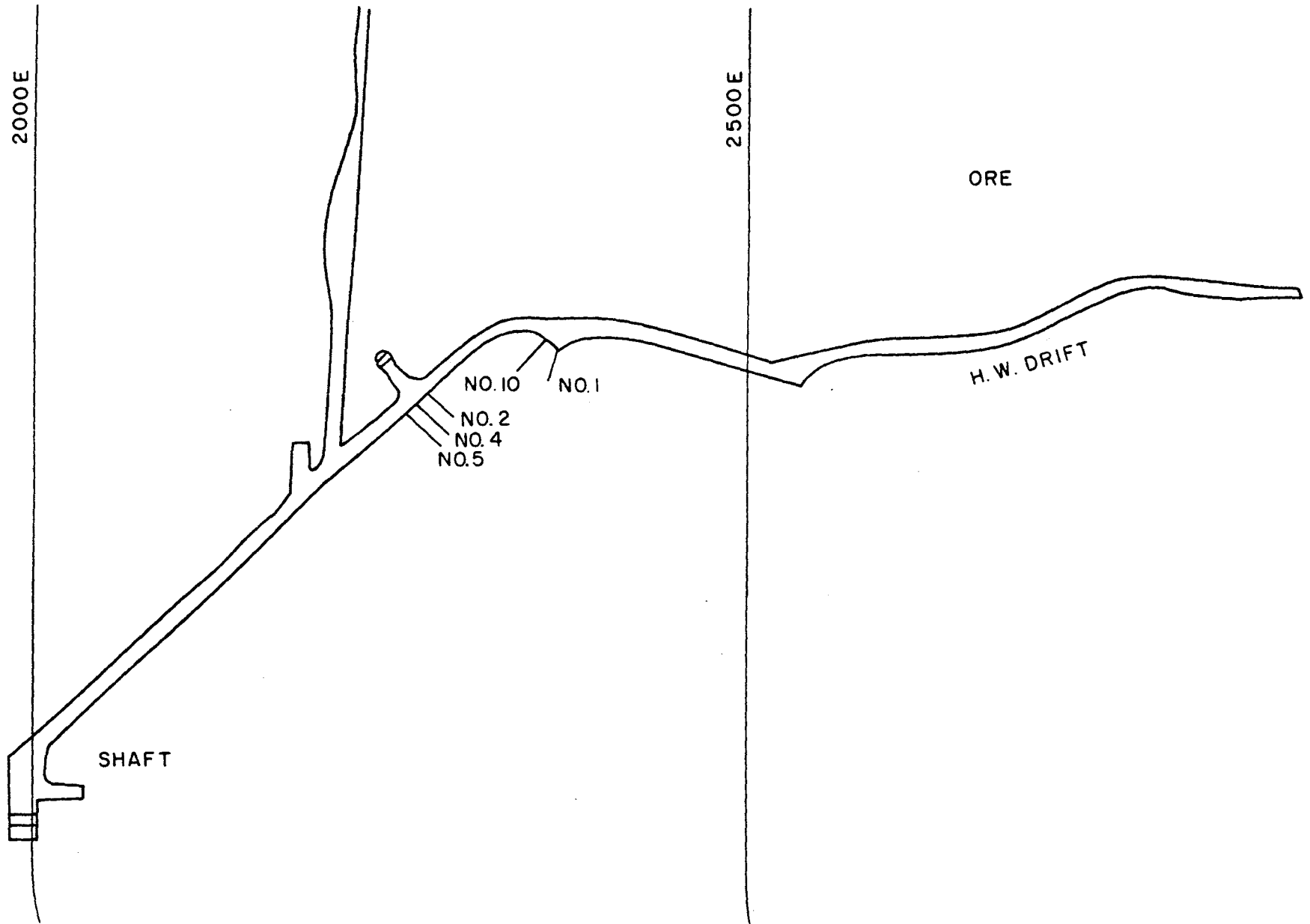


Figure 7. Location of field stress holes in iron mine B.

Hole No. 2 was drilled in metadiorite, which contained chloritic coatings along the partings and joint planes. This hole was drilled almost perpendicular to strike. Hole Nos. 4 and 5 were drilled parallel to Hole No. 2. Measurements were taken in these holes to obtain information on the reproducibility of data using this technique.

Hole No. 10 was drilled perpendicular to Hole No. 2. The rock was composed mainly of calcium carbonate with some magnesium carbonate and siderite. The rock was found to be free from lineations. Hole No. 12 was drilled on the same level, parallel to strike but near the section containing pillar 42.

The results for Holes No. 1, 2, 4, 5, 10 and 12 are shown in Table 8. Each stress value is the average of many readings obtained at that location. They indicate that parallel to strike the horizontal field stress is of the order of 4000 psi, with the vertical stress being of the order of 3000 psi. In the horizontal direction perpendicular to strike and more or less perpendicular to the orebody, the measurements vary; it is possible that the different depths might account for some of the difference.

The results of these overcoring measurements show considerable variation, which either may be a faithful representation of the field stress conditions or may be due to the technique, banding in the formation, and presence of joints in the rock mass. Some of the results are known to have been affected by joints located at critical positions with respect to the overcoring operation. However, when more information on this general subject is obtained, it will probably be found that assuming the presence of homogeneous stress fields may seldom be valid.

The measurement of vertical stresses in some of the holes greater than the overburden stress (approximately 1500 psi) can only be explained by a mechanism of crustal movement producing stresses greater than gravity through shear transfer from adjacent zones. The presence of higher horizontal stresses, of course, must also be explained by crustal movement.

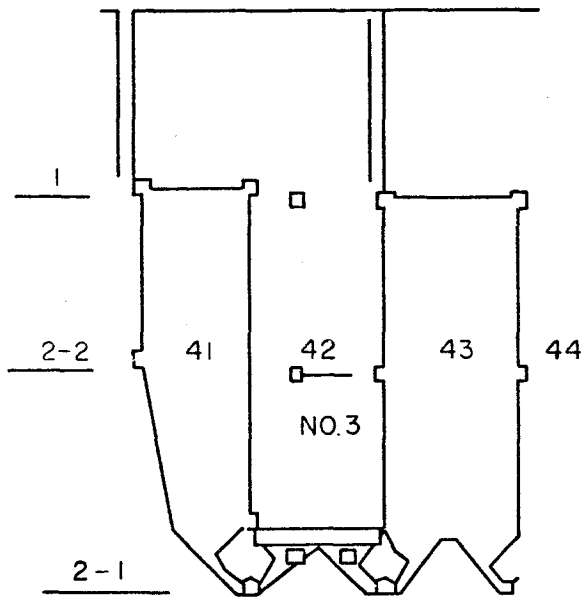
Overcoring was conducted in the 42 pillar in the central part of the 2-2 sub-level as shown in Figure 8. Figures 9 and 10 show the geological section through this pillar, and Figures 11 and 12 the geological plans for the pillar.

The hole was drilled horizontally 13 ft parallel to strike towards the 43 stope. The depth below the ground surface of the sub-level was about 1400 ft. Beyond the 43 stope, the 44 pillar and the 45 stope had been mined out; further to the east is a dike which forms, in effect, a permanent pillar. Beyond the 41 stope a metadiorite intrusion eliminated any mining for about

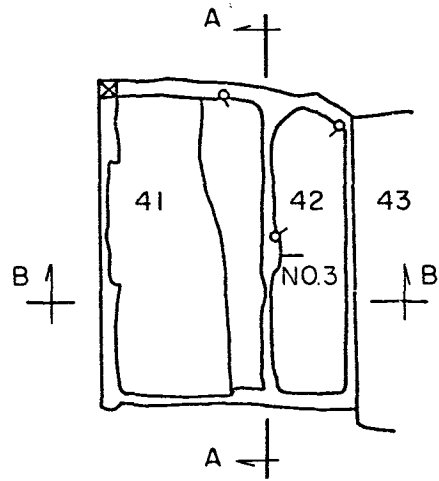
TABLE 8

Experimental Data from Iron Mine B (10)N = 1, R = 0.80, $\mu = 0.16$

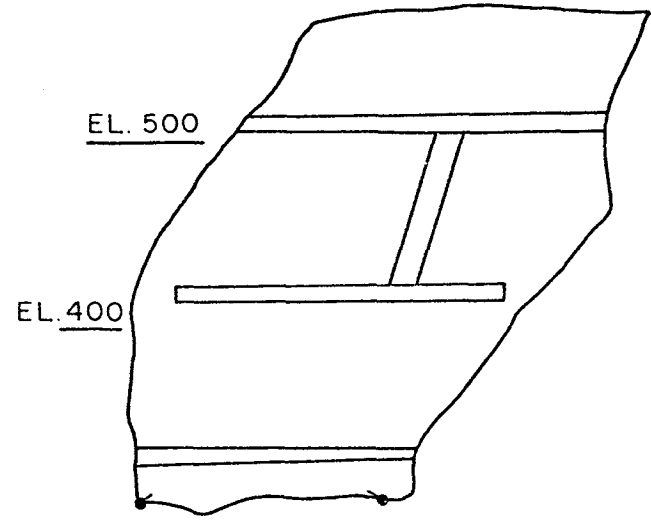
No.	L	H	B	z	x	i	S _v	S _o	S _t	σ_p
	ft	ft	ft	ft			psi	psi	psi	psi
G-1	-	-	-	1260	-	-	2430	-	-	-
G-2	-	-	-	1260	-	-	2690	-	2625	-
G-3	326	200	66	1400	0.35	64°	935	-	-	2640
G-4	-	-	-	1260	-	-	3220	-	4350	-
G-5	-	-	-	1260	-	-	3420	-	3920	-
G-6	360	175	60	1125	0.47	50°HW 90°FW	1230	-	-	2950
G-10	-	-	-	1260	-	-	1400	1370	-	-
G-12	-	-	-	1600	-	-	1180	2130	-	-



SECTION B-B



PLAN AT 2-2 SUBLEVEL



SECTION A-A

Figure 8. Plan and sections, Pillar 42.

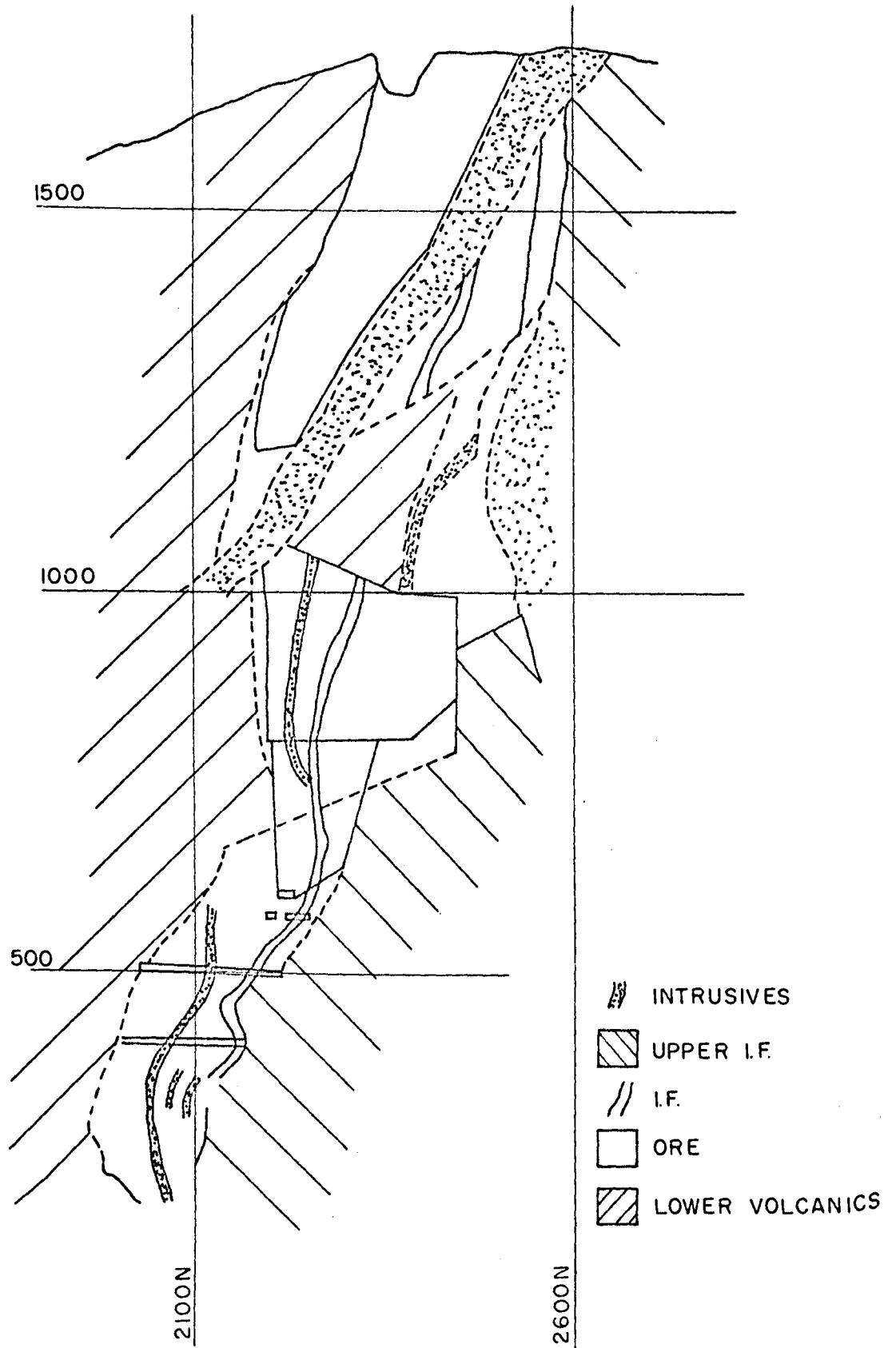


Figure 9. Geological section of mine through Pillar 42.

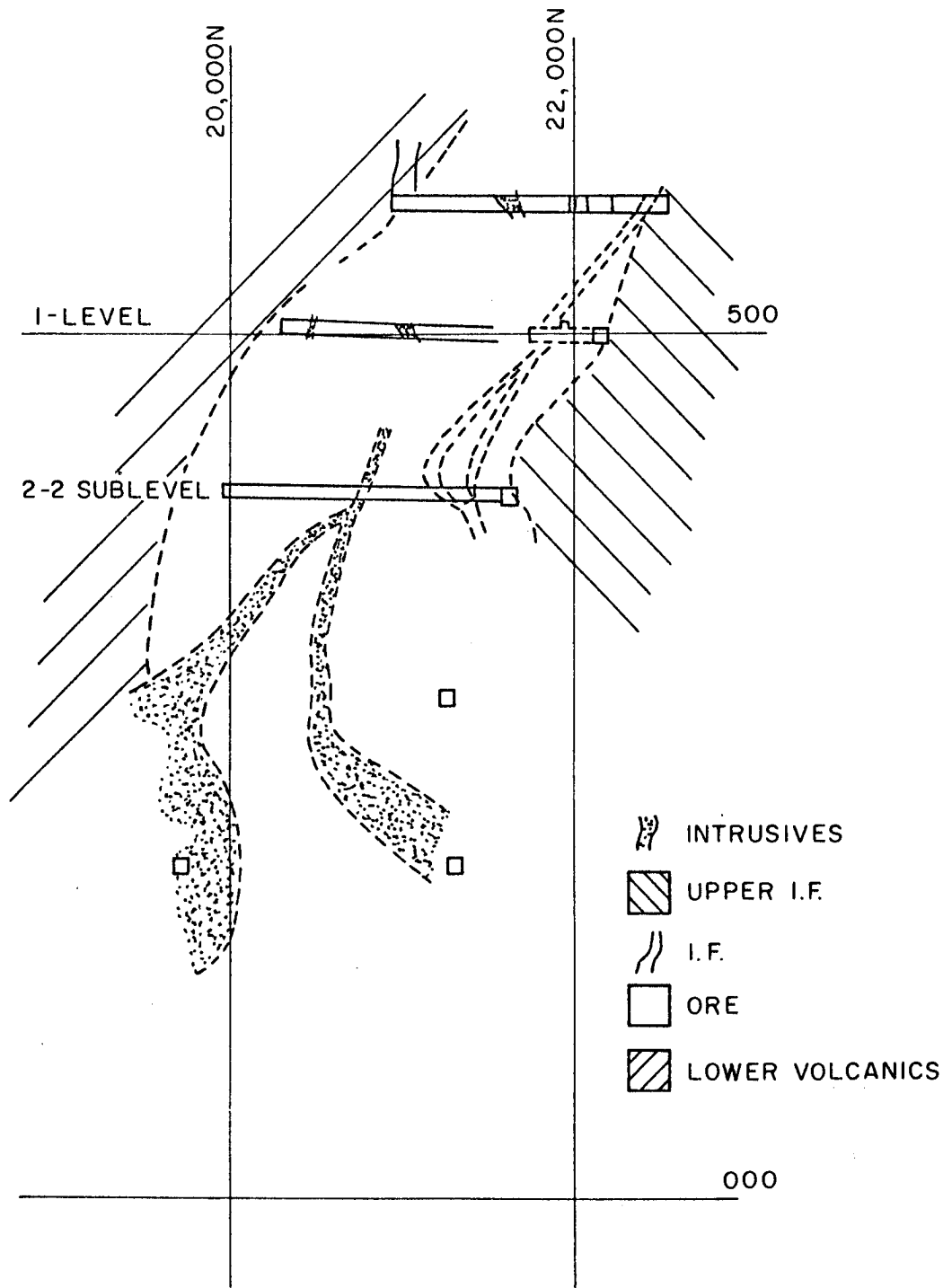


Figure 10. Geological section of Pillar 42.

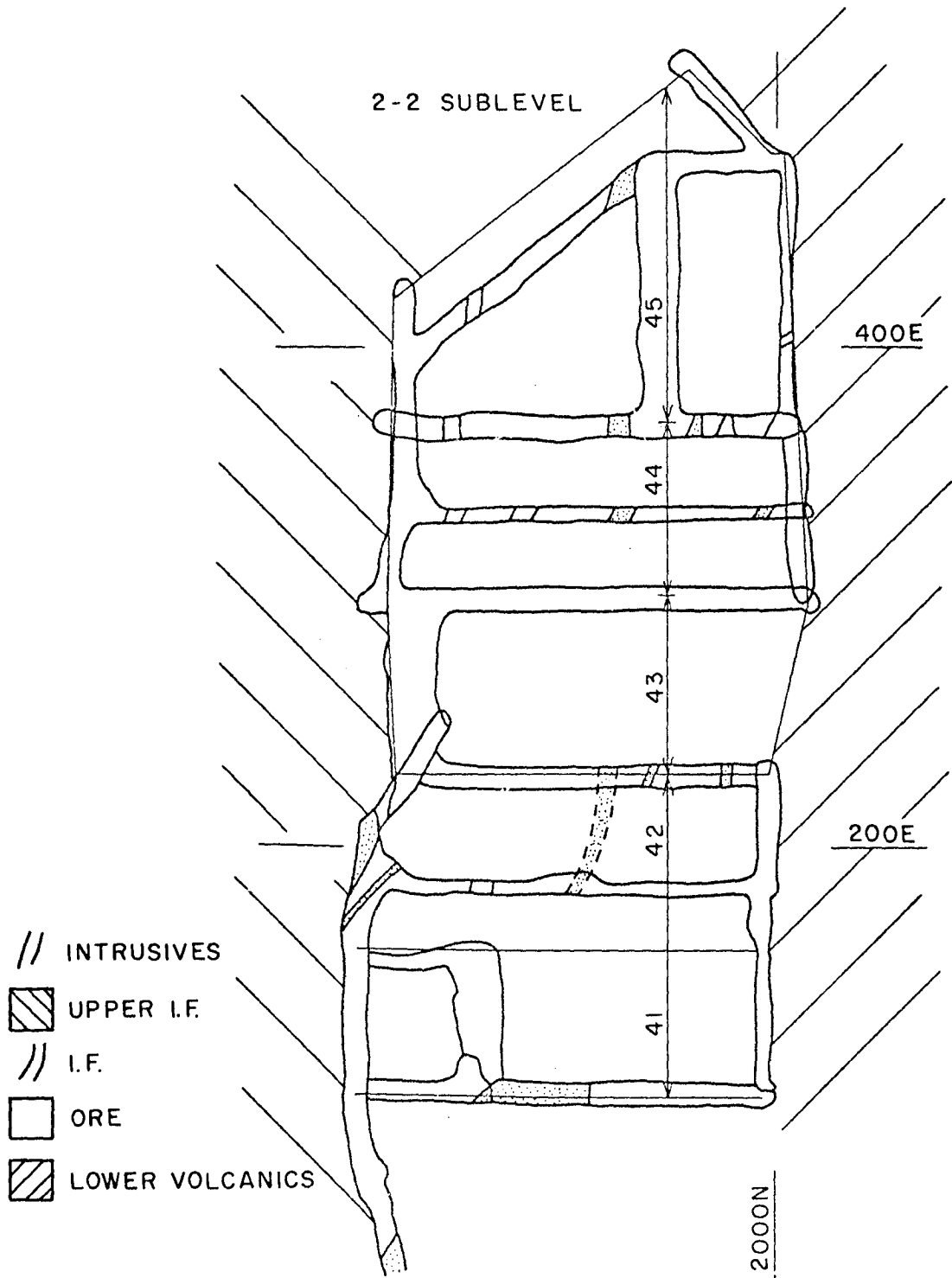


Figure 11. Geological plan of Pillar 42, 2-2 Sublevel.

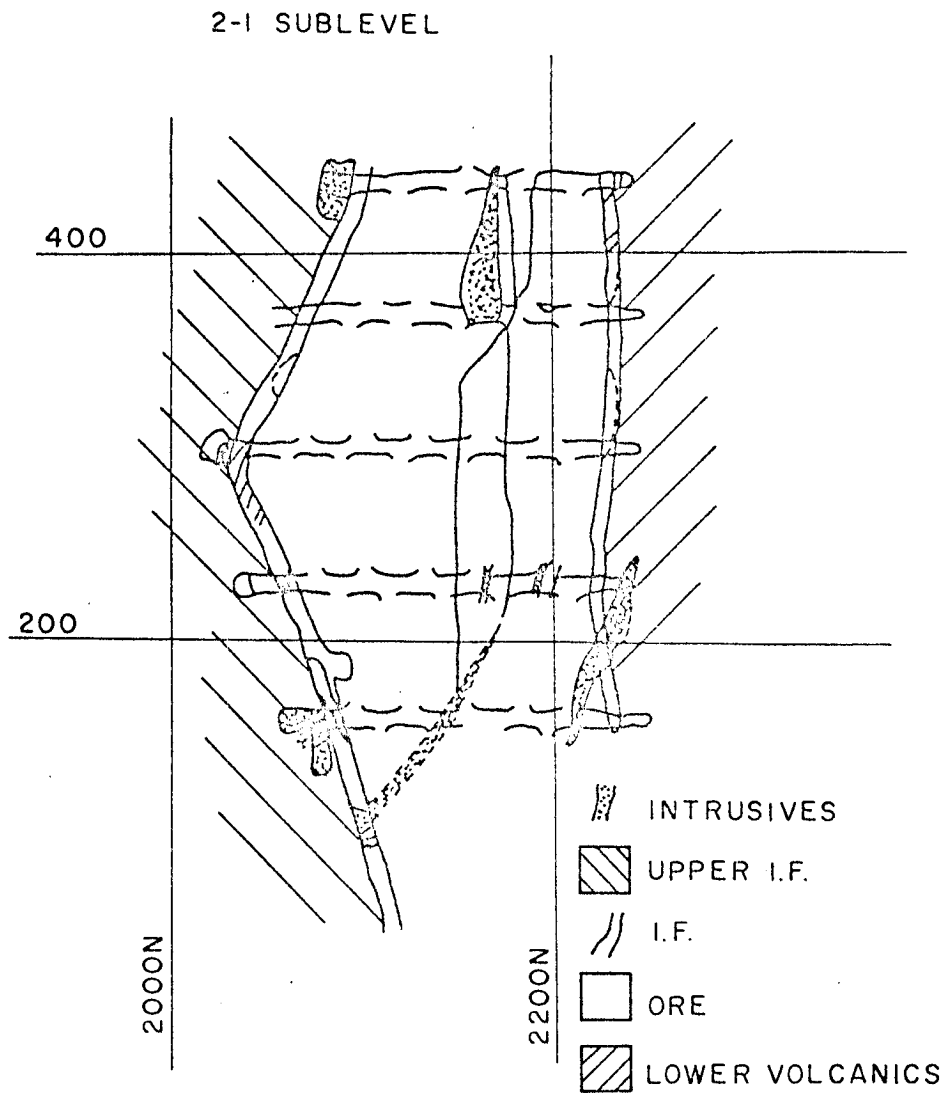


Figure 12. Geological plan of Pillar 42, 2-1 Sublevel.

300 ft on strike. The stopes above had all been mined out previously.

The results of these measurements (Hole No. 3) are given in Table 8. The measurements indicated that the major principal stress was acting very close to perpendicular to the walls.

Measurements were also made in the 51 pillar. This pillar, as shown in Figure 13, had a breadth of 60 ft, a length of 280 ft downdip, and a thickness of 175 ft between walls. Figure 14 shows the geological section through the pillar, and Figure 15 shows geological plans.

Before the stress measurements were made, the blocks 48, 49 and 50 had been mined out to the west and stope 52 to the east had just been completed. The measuring site was substantially midway between the walls, with Hole No. 6 being drilled eastward.

The results (Hole No. 6) are shown in Table 8. Again the measurements showed the major principal stress to be substantially perpendicular to the walls. The pillar stress of 2950 psi is substantially the same as obtained in the 42 pillar. Although the geometries associated with these two pillars are not identical, they are very similar since both had three blocks excavated on one side and one block on the other with the measurements being taken at an elevation within 90 ft of each other. Consequently, other things being equal, the results should be substantially the same.

Analysis of Data. It was seen above, in Table 8, that the field stress at the measuring station away from the stoping areas is probably not homogeneous. In addition, a satisfactory measurement of the field stress normal to the orebody was not obtained. However, to permit trial calculations from the measurements obtained, it is assumed that the horizontal field stress parallel to strike, S_t , is 4000 psi and that the average field stress normal to the orebody, S_o , at the level of the pillar holes is 1600 psi.

In using the field stress measurements in the hypothesis, it could be assumed either that the major principal field stresses were constant in direction with respect to the north-south datum or that they were constant in direction with respect to the strike of the orebody. In this work it was assumed that the directions would remain constant with respect to the orebody, so that the stresses parallel and perpendicular to strike at the measuring station would be also parallel and perpendicular to strike in the stoping areas.

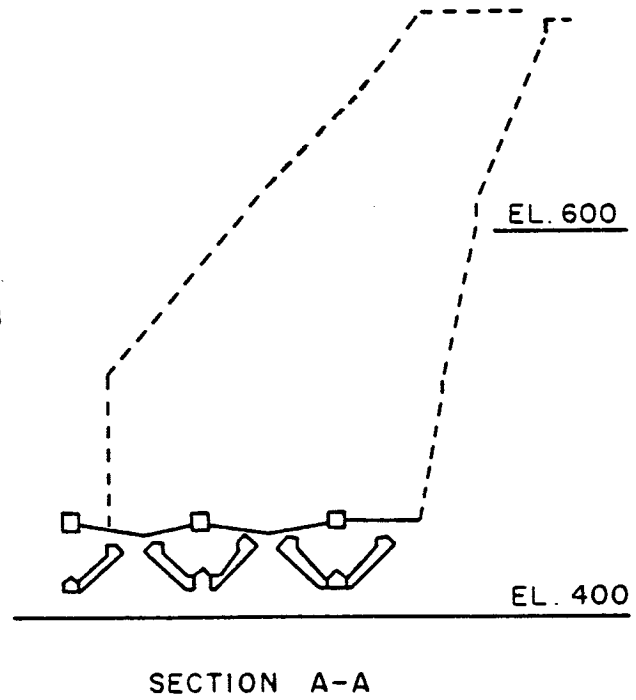
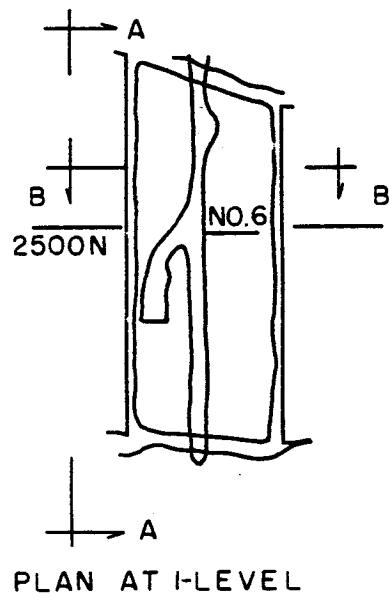
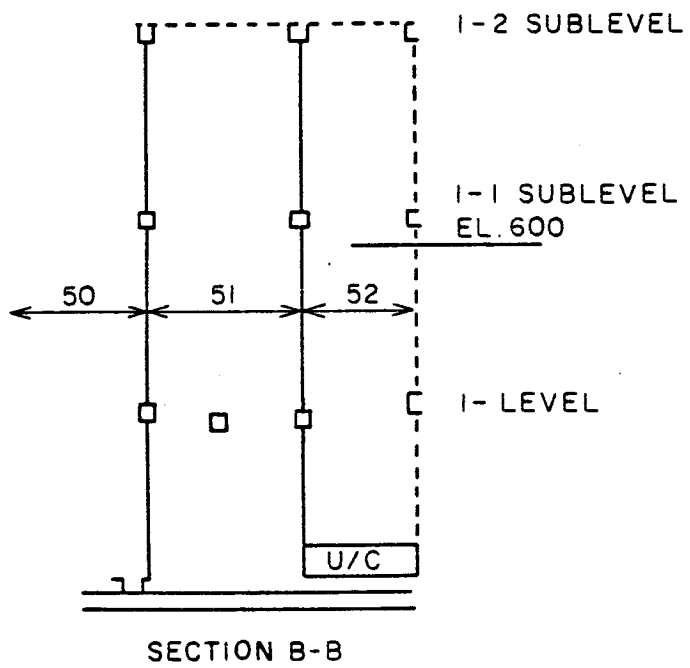


Figure 13. Pillar 51, plan and sections.

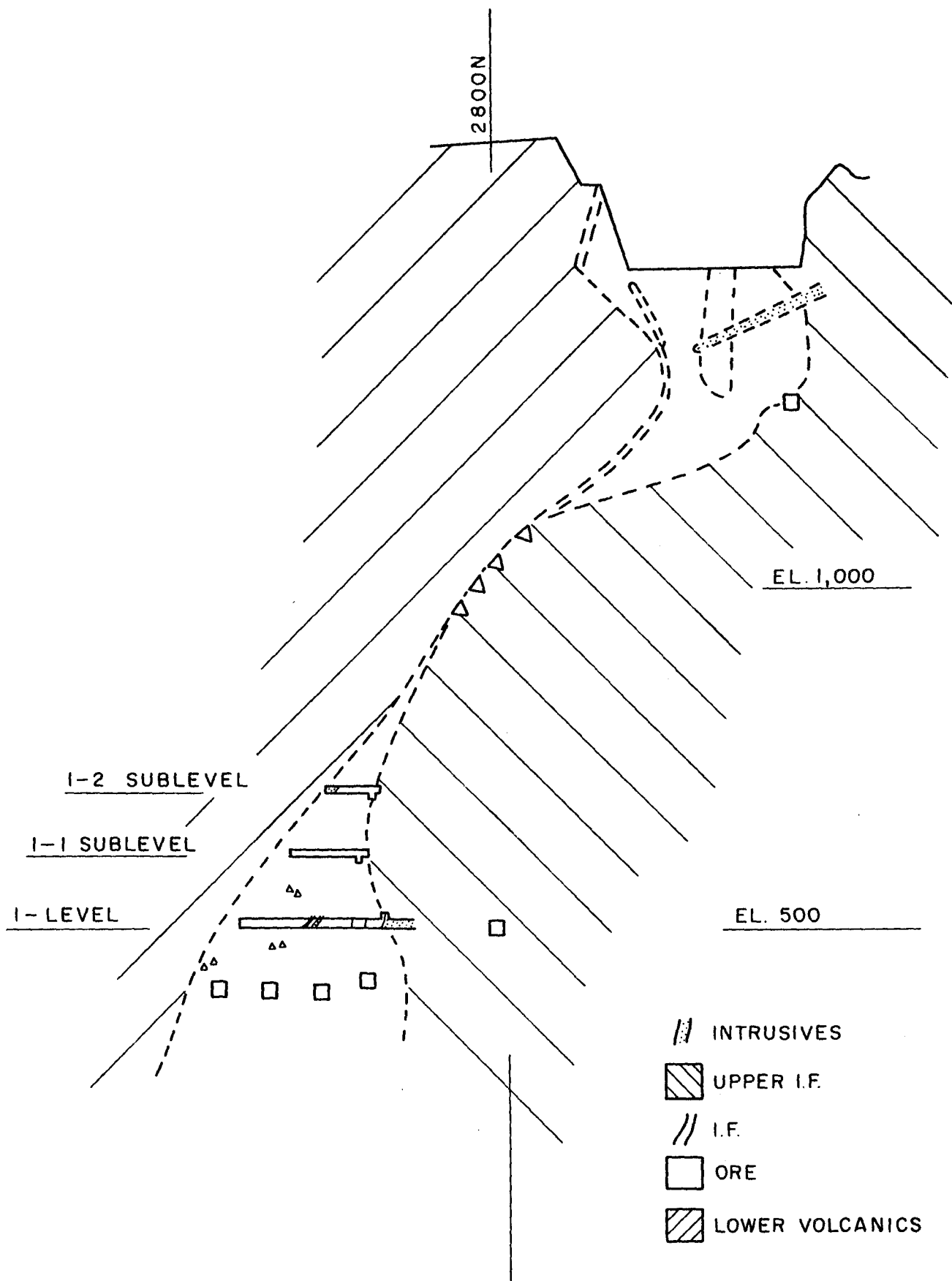


Figure 14. Geological section through Pillar 51.

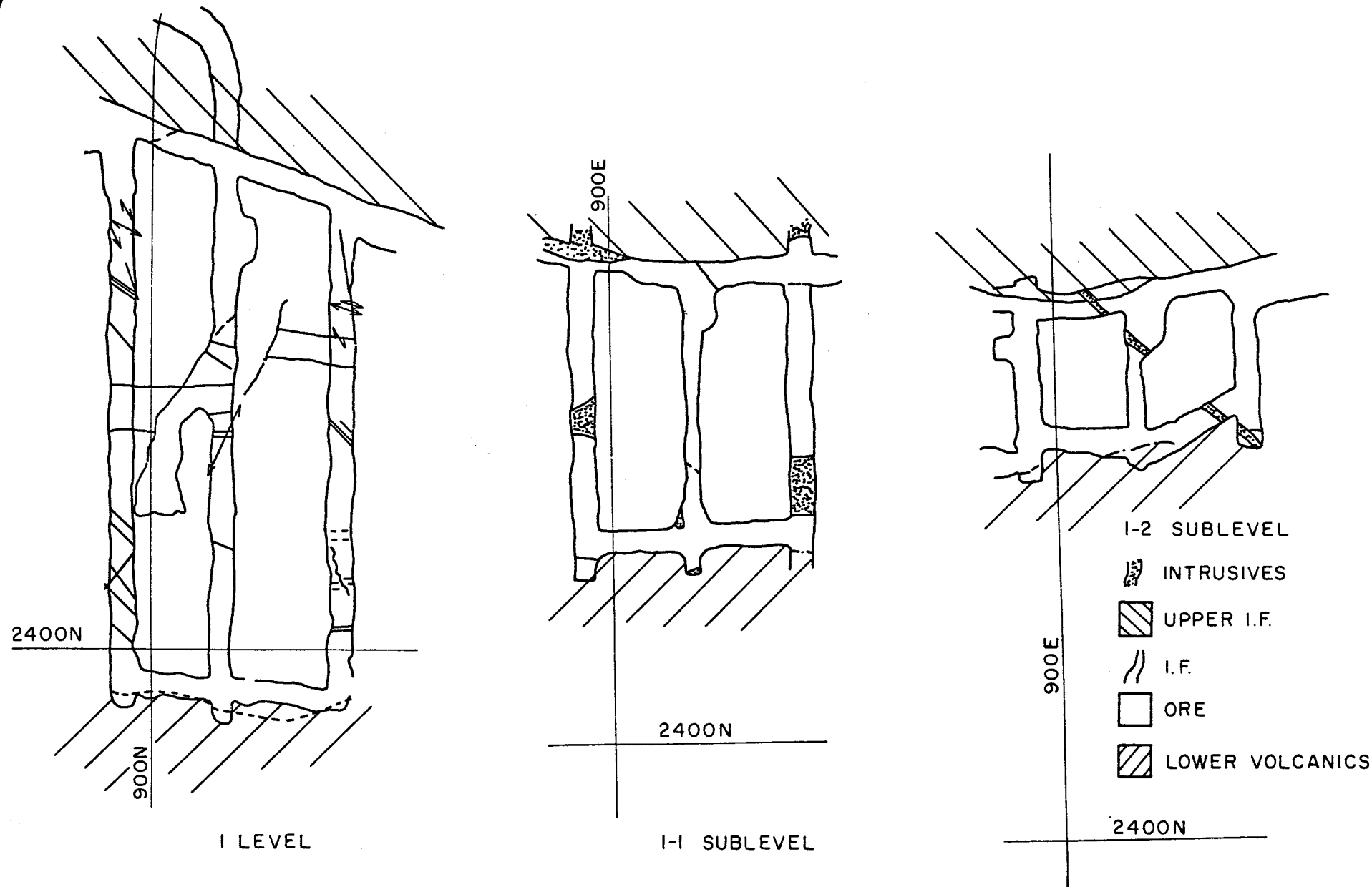


Figure 15. Geological plans of Pillar 51.

The deformation properties of the pillar and wall rocks were obtained from tests on core samples. Whereas these tests provide a measure of the properties of the rock substance, it is to be questioned whether the rock mass has the same properties. Usually, it could be assumed that the rock mass would have a lower modulus of deformation than the rock substance, and that Poisson's ratio would also be lower for the rock mass than for the substance. In spite of these possibilities, only laboratory data could be obtained. Based on these tests it was assumed that the parameter n was equal to 1 and that Poisson's ratio for both the pillar and wall rocks was equal to 0.16. The tests indicated that the rock substance in the pillars had a higher modulus of deformation than did the rock substance in the walls. However, field measurements of strain, in the pillars, resulting from stoping in the adjacent blocks and also from taking a slash off a pillar, indicated that the pillar rock worked to some extent as a result of the increased stresses, so that the material was less competent or had a lower modulus of deformation than in its undisturbed state (10). Consequently, it is possible that the parameter n was actually greater than 1; however, the techniques for obtaining an accurate measure of the rock properties for this parameter have yet to be developed.

In Table 9 the analysis of the data is presented. The measured pillar loadings, according to these calculations, are less than those predicted by the tributary area theory and somewhat less than those predicted by the hypothesis. The bases for the parameters in these calculations, as explained above, are not perfectly satisfactory. However, even if the assumptions on material properties and field stresses were correct (and S_0 is a critical parameter), the basic assumption in the hypothesis of a long mining zone would still not be fulfilled. By recognizing that the lengths of the stopes down-dip were not infinite, in other words taking into account the three-dimensional aspects, which would decrease deflections, it would be found that the predicted pillar stresses where measurements were made would be less than shown in Table 9.

TABLE 9

Analysis of Data from Iron Mine B

$$N = 1, k = 2.5, \mu = 0.16, n = 1$$

No.	R	h	b	x	$\Delta\sigma'_p$	$\Delta\sigma'_p$	$\Delta\sigma'_p$
					MEAS	TA	HYP
G-3	0.80	0.61	0.20	0.35	0.63	2.00	0.74
G-6	0.81	0.49	0.19	0.47	0.82	2.13	0.92

Uranium Mine

General Geology. The uranium mine occurs within the Pre-Cambrian Huronian formation. The Huronian rocks were deposited on a major unconformity which was eroded flat except for some softer volcanics that produced small depressions in the northwest-southeast direction. The Huronian formation containing the ore is a river deposit forming a monolithic quartzite some 700 ft thick at the mine site, decreasing in thickness to the north and increasing to the south. The vein is generally 6 ft to 12 ft thick and lies 30 ft to 40 ft above the pre-Huronian erosion surface. As a rule the Huronian rocks here are only gently folded and slightly metamorphic (11, 12).

At the mine site the formation has been folded into a broad syncline with an east-west axis plunging gently to the west, as shown in Figure 16. The mine is on the south limb of the syncline and is worked from the surface down to the 1400-ft level.

Faults occur regionally, with strikes in the northwest and northeast directions. In addition, there is a main east-west fault. The movement has generally been from the south up and to the west.

The formation is cut by several east-west, wide diabase dikes having an almost vertical dip. Some diabase sills were formed at the same time. At a later time some thin (less than 1 ft) basic dikes were intruded.

Structural Geology. As a result of compression from the south, the whole region was formed into broad open folds. The axis of the local fold plunges 5° west. The vein in the mine area has generally a dip of between 13° and 18° north with an almost east-west strike, as shown in Figure 17. However, at the stopes in which the pillar stresses were measured, the dip varied locally from 10° to 25° (12).

The dikes actually range from narrow stringers to about 100 ft wide and in many cases are consistent over several miles of strike.

Numerous faults intersect the ore horizon. The displacement of these faults is rarely more than about 30 ft. In the test area no faults were detected. However, in the mine itself, faults have been identified which generally strike about N 75 E, dipping steeply north with, so far as can be detected, less than about 1 ft of displacement downthrown to the north.

The joints examined in the mine are usually normal to the bedding. Their strike is generally N 80 W to N 85 W. They occur in groups and seldom seem to extend for more than about 75 ft. Some were observed striking N 75 E to N 80 E; this may be associated with faulting.

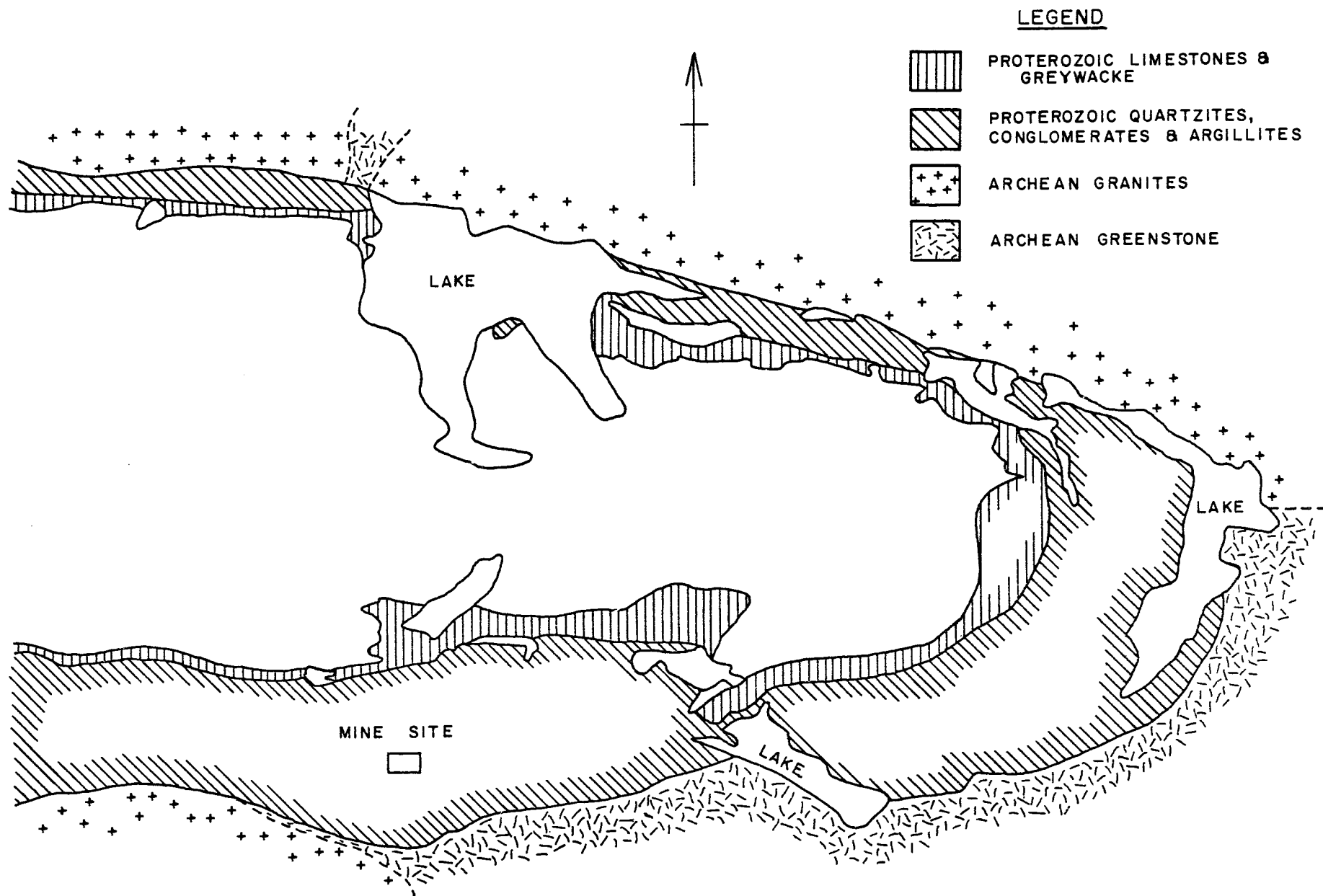


Figure 16. Regional geology of uranium mine area.

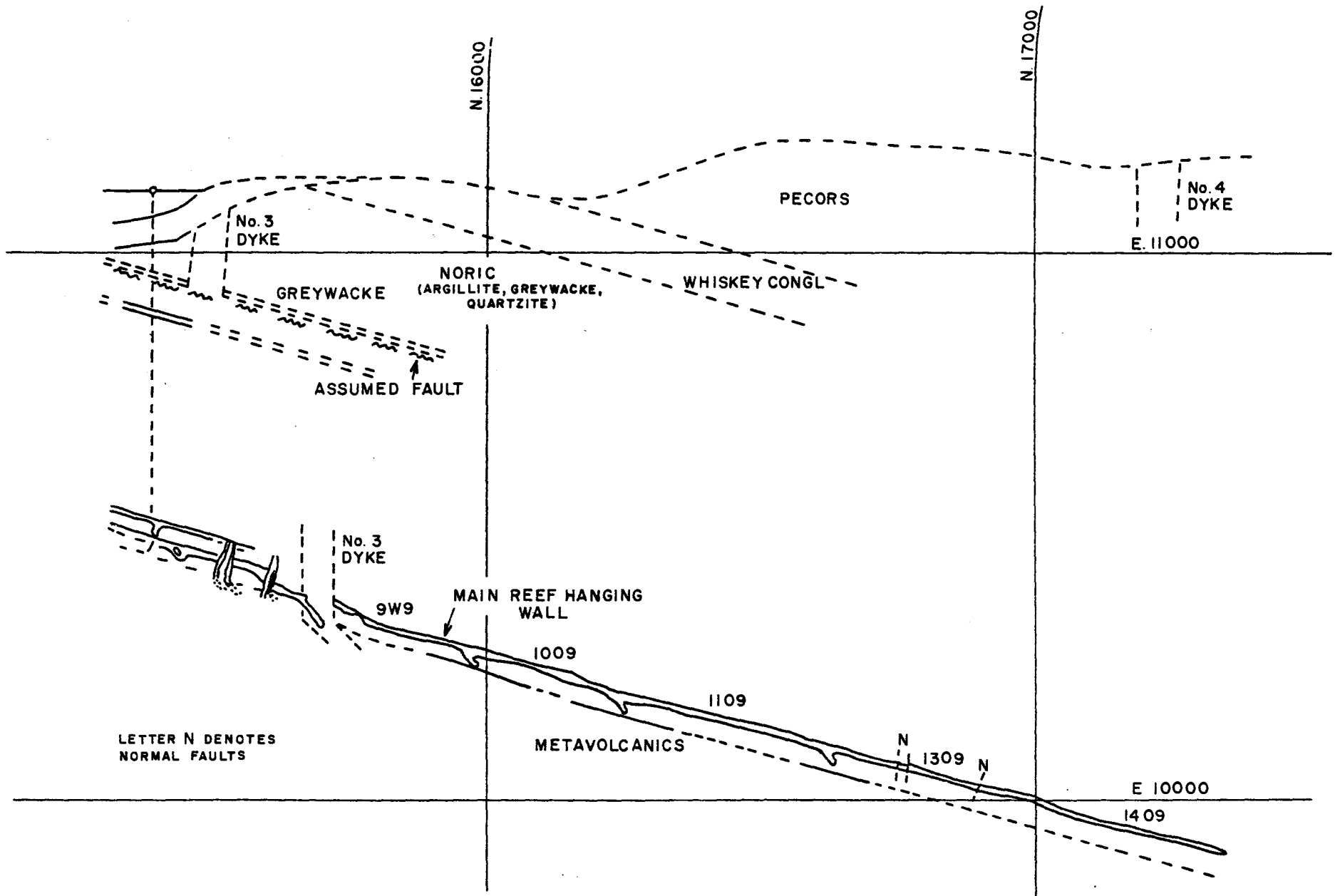


Figure 17. Vertical geological section through uranium mine.

Lithology. The ore generally occurs in closely packed conglomerate with a pyritic matrix and is most often found towards the hangingwall and the footwall. The close-packed conglomerate grades into loose-packed conglomerate with streaks of pyrite and in some cases no pyrite. The matrix of all the conglomerate is quartzite (12).

The pebbles of the conglomerate are generally quartz, with occasionally some black chert. The pebbles are generally between 0.5 and 2 in. in diameter and generally rounded to sub-rounded. However, some angular fragments and obviously crushed pebbles can also be seen.

The quartzite beds are as much as 5 ft thick, with grain sizes of $\frac{1}{2}$ mm to 2 mm. The grains are sub-round, closely packed, and cemented with sericite. A small amount of microcline occurs in the matrix.

The matrix of the loose-packed conglomerate has the same strength characteristics as the pebble-free quartzite. The strength of the close-packed conglomerate may decrease with increasing pyrite content. However, because the pyrite is not concentrated in single layers, it is difficult to predict differences in mechanical properties from geological considerations alone.

The main diabase dike to the south of the test area is massive, fine to medium grained, has a width of 60 ft, and dips about 80° to the south. The ore vein in the adjacent areas rolls down on the south side and up on the north side. In this area, normal faulting has been concentrated south of the dike. The dike rock has not been altered and hence forms a competent barrier.

Mining. The stope configuration is a conventional room and pillar pattern, as shown in Figure 18. Haulageways are driven on strike, providing stope lengths between 200 ft and 350 ft. Rooms are turned off up-dip, with a central pillar, 10 ft wide, extending up-dip and two 65-ft stopes on either side of this central pillar. These stopes are separated from the adjacent rooms by 10-ft rib pillars. A crown pillar nominally 15 ft in breadth is left between the top of the rooms and the next haulage-way (11).

To commence stoping, twin raises are driven on either side of the central pillar from one level to the next. The face is then advanced by slashing the outer wall of the raise outward from the bottom up.

Method of Measurement. The method of measuring the pillar and field stresses in this mine was the same as used in Iron Mine B.

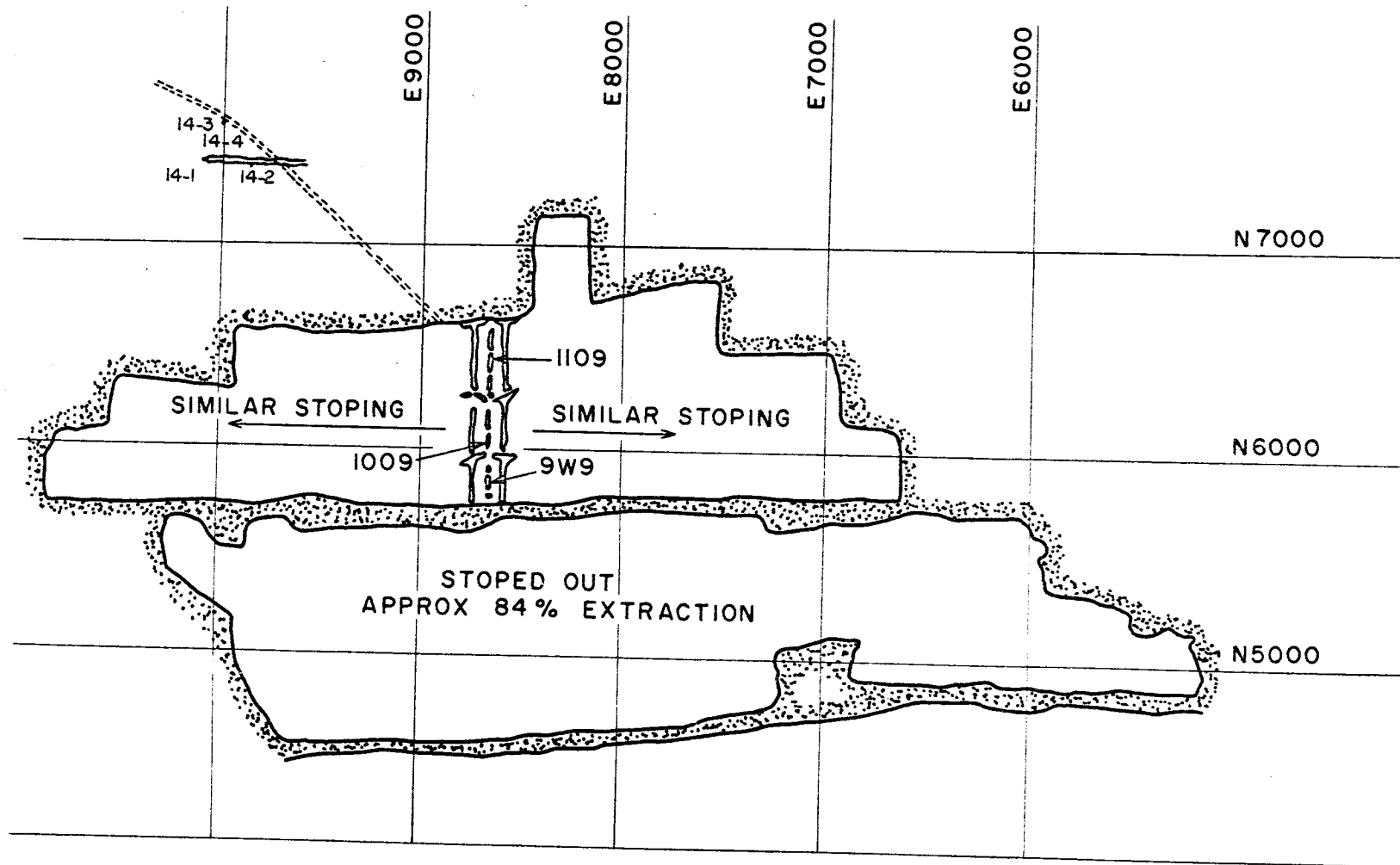


Figure 18. Plan of uranium mine.

Experimental Results. The results of the measurements of pillar stresses and field stresses in this mine are shown in Table 10. The general extraction ratio, R , is equal to the local extraction ratio, r , owing to the large number of pillars and the regularity of the stope layouts throughout the mine. The height of the pillars, H , is an average figure. The ratio of the moduli of deformation of pillar rock to wall rock, n , and Poisson's ratios, μ and μ_p , for wall rocks and pillars were obtained from tests on the rock substance (11).

The pillar stress measurements shown in Table 10 are the average results from several readings varying from 3 to 9 deformation readings in each hole. The field stress values are representative of several readings varying from 14 to 25 deformation measurements in each hole. Holes 14-1 and 14-4 were drilled parallel to strike and thus measured stresses in the plane perpendicular to strike; 14-2 and 14-3 were drilled perpendicular to strike and thus measured stresses in the vertical plane parallel to strike.

Figure 18 shows the plan of the uranium mine with the boundaries of the mined-out zone at the time of the measurement of stresses. The mine is divided by vertical diabase dikes, one of which is shown at the bottom of the plan and another of which runs through the central part of the mine just south of the N 6000 co-ordinate. The north abutment of the mining zone contained the active working faces. Pillar stress measurements were conducted in the stopes shown in detail in Figure 18, i. e., 9 W 9, 1009 and 1109. The field stress measurements were conducted in drifts as far away from the mining zone as possible, as shown in Figure 18 in holes 14-1 to 14-4.

Figure 19 shows the plan of stope 9 W 9. The pillars were designated left, central and right while looking up-dip. Three overcoring holes were drilled in both the left and right pillars, and two were drilled in the central pillars. This plan also shows the fracture or joint lines that could be observed in the roof of the stope.

Figure 20 shows the plan of stope 1009. In this stope two overcoring holes were drilled in each of the left, central and right pillars. As can be seen from this figure, the frequency of joints or fractures was much less than in 9 W 9 stope.

Figure 21 shows the plan of stope 1109. In this stope two overcoring holes were drilled in both the left and right pillars. Three overcoring holes were drilled in the central pillars. The frequency of joints or fractures was much greater in this stope than in either the 9 W 9 or the 1009 stope.

TABLE 10

Experimental Data from Uranium Mine (10)

$R = 0.84 = r$, $L_1 = 900$ ft, $L_2 = 2000$ ft, $H = 10$ ft, $\mu = 0.16$, $i = 14^\circ$

No.	B	z	x_1	x_2	S_h^y	S_v	S_o	S_t	σ_p
	ft	ft				psi	psi	psi	psi
9-1R	9.4	870	0.62	0.27	-	-	-	-	disced
9-2R	8.3	860	0.76	0.21	-	-	-	-	8,200
9-3R	7.7	850	0.89	0.15	-	-	-	-	10,300
9-1L	14.5	870	0.62	0.27	-	-	-	-	7,700
9-2L	8.7	860	0.76	0.21	-	-	-	-	7,630
9-3L	10.7	850	0.89	0.15	-	-	-	-	13,700
9-1C	10.7	870	0.62	0.27	-	-	-	-	5,480
9-2C	8.8	860	0.76	0.21	-	-	-	-	disced
10-1R	10.2	910	0.09	0.51	-	-	-	-	7,270
10-2R	15.2	890	0.33	0.40	-	-	-	-	8,010
10-1L	14.8	910	0.09	0.51	-	-	-	-	6,840
10-2L	14.2	890	0.33	0.40	-	-	-	-	6,340
10-1C	8.7	910	0.09	0.51	-	-	-	-	12,260
10-2C	9.7	890	0.33	0.40	-	-	-	-	8,150
11-1R	8.3	1000	0.67	0.25	-	-	-	-	disced
11-2R	13.6	980	0.44	0.35	-	-	-	-	10,460 ^x
11-1L	13.6	1000	0.67	0.85	-	-	-	-	9,190
11-2L	10.7	980	0.44	0.75	-	-	-	-	10,580
11-1C	8.2	1010	0.73	0.88	-	-	-	-	10,210
11-2C	11.2	990	0.53	0.79	-	-	-	-	9,320
11-3C	20.3	960	0.27	0.67	-	-	-	-	10,230
14-1	-	1280	-	-	-	2520	2470	4390	-
14-2	-	1280	-	-	4210	2150	-	-	-
14-3	-	1360	-	-	4950	2870	-	-	-
14-4	-	1360	-	-	-	2480	2570	2990	-

^xUnreliable readings.

^yHorizontal field stress parallel to strike.

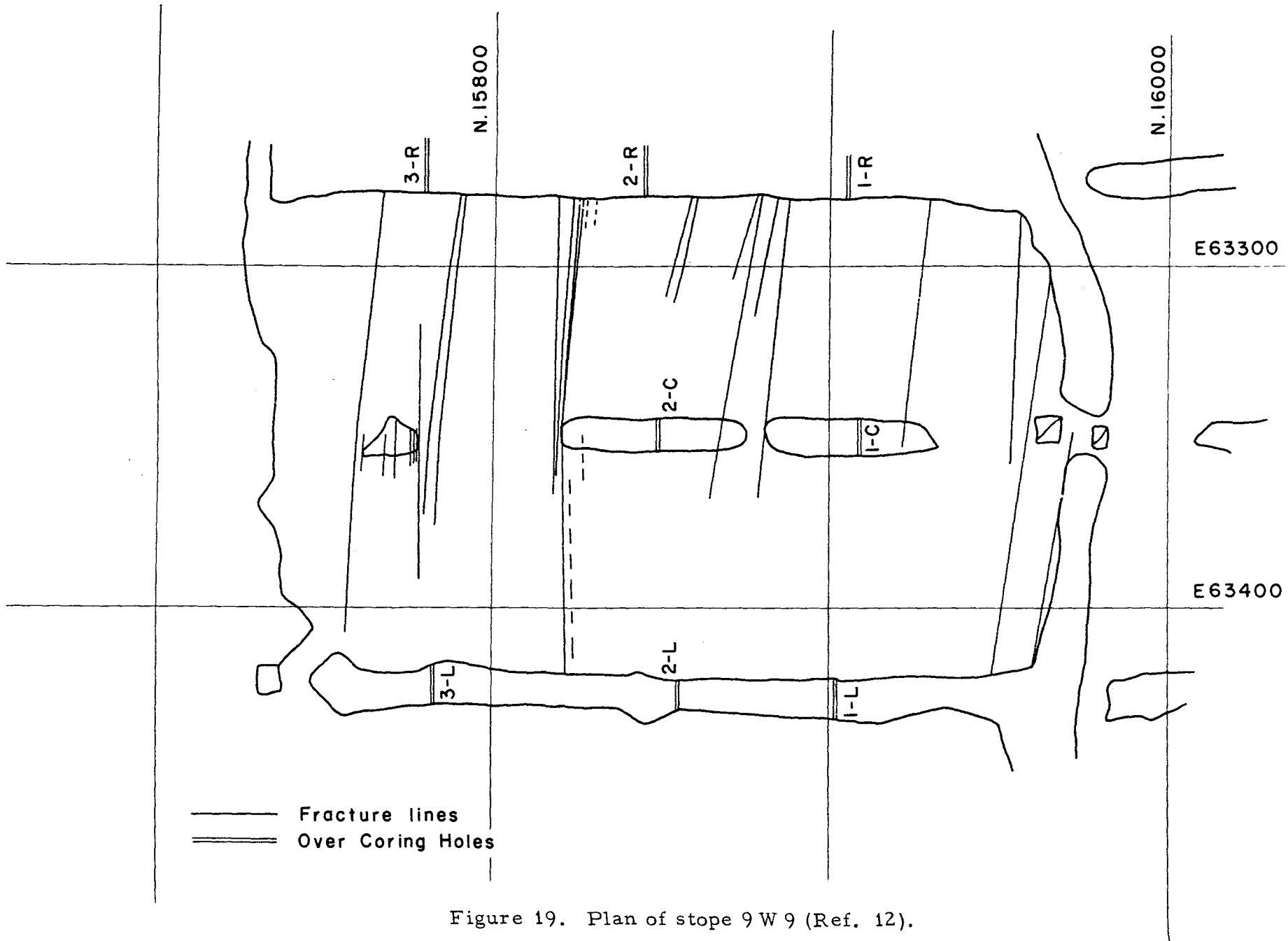


Figure 19. Plan of stope 9 W 9 (Ref. 12).

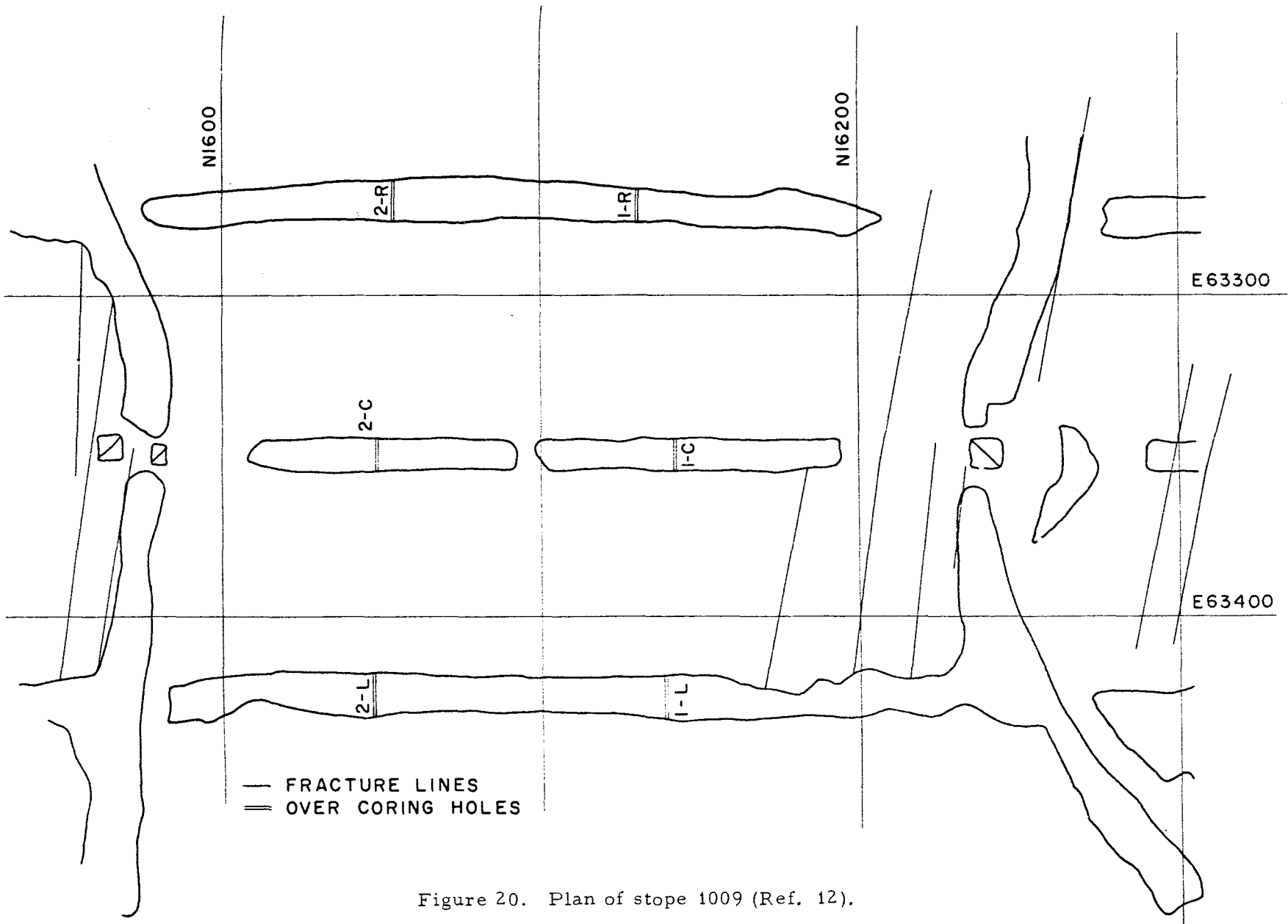


Figure 20. Plan of stope 1009 (Ref. 12).

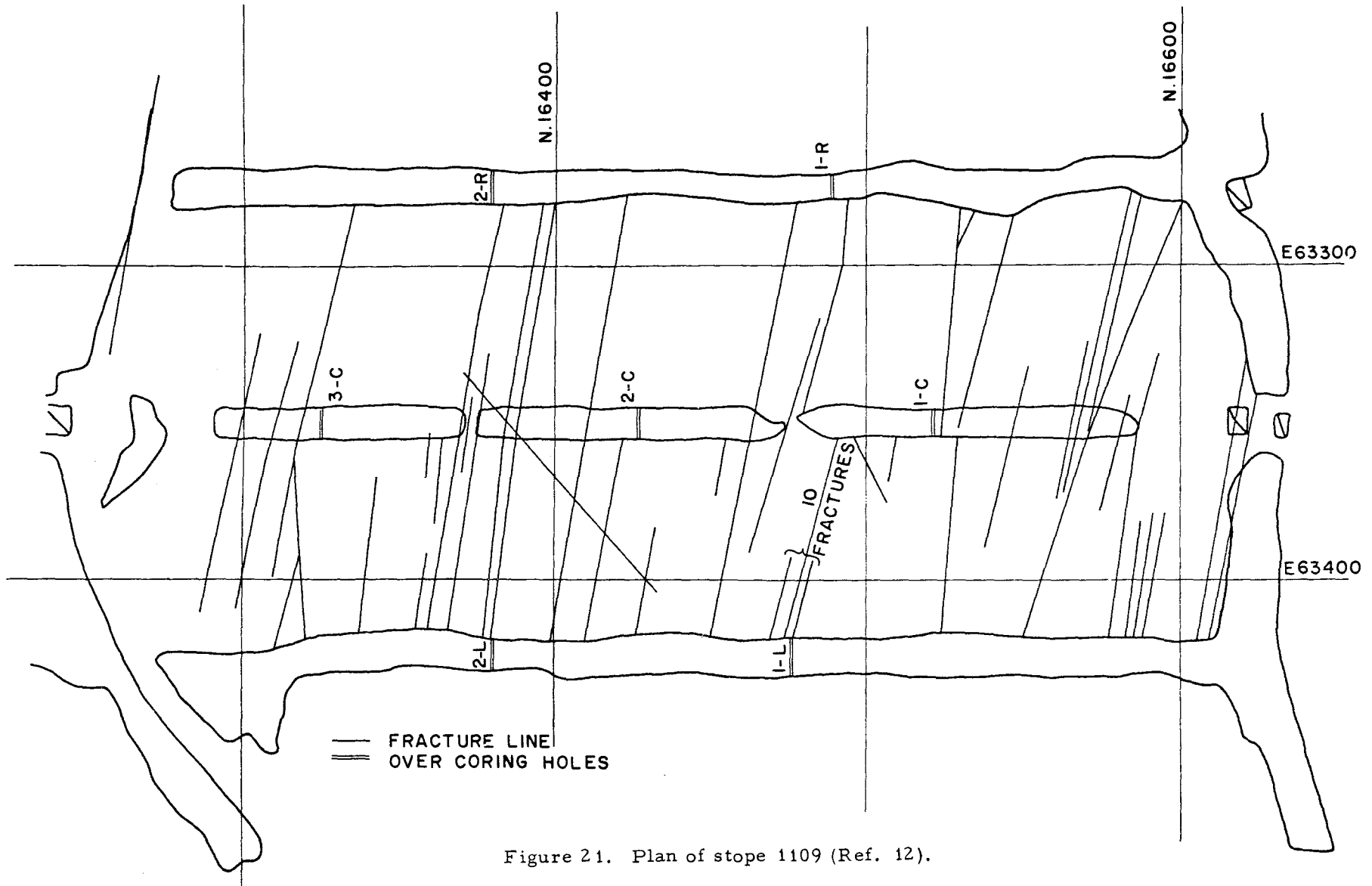


Figure 21. Plan of stope 1109 (Ref. 12).

Figure 22 shows the vertical section of the west or right rib pillar in the 9 W 9 stope. The conglomerate bands in the quartzite country rock are indicated in this section, together with fracture lines in the pillar.

Figure 23 is a vertical section showing the centre pillar in the 9 W 9 stope. Conglomerate bands and fracture lines in this pillar are shown on the section.

Figure 24 shows a vertical section of the east or left rib pillar in the 9 W 9 stope. This section shows the pronounced increase in dip angle at the left side of the section, which is adjacent to the central diabase dike.

Figure 25 shows a vertical section of the west or left rib pillar of the 1009 stope. As in the case of the plan showing the joints in the roof, this section indicates that there were practically no joints or fracture lines visible in the pillar.

Figure 26 shows a vertical section of the centre pillar in the 1009 stope. Again very few fracture lines could be seen in these pillars.

Figure 27 shows a vertical section of the east or left rib pillar in the 1009 stope. No fracture lines are observed on the surface of this pillar.

Figures 28, 29 and 30 show the vertical sections of three pillars in 1109 stope. As indicated by the plan of this stope, the frequency of fracture lines in the pillars was much greater than for either of the two previous stopes.

The sites at which the measurements of field stresses were made were 900 ft to 1100 ft away from the mining zone. This distance would be adequate to avoid any stress concentration effects around the stopes if the span of the mining zone was 900 ft, i. e., the distance from the north abutment to the central dike just south of the 9 W 9 stope as shown in Figure 18. However, if the effective span of the mining area was to the next dike at the south side of the mining zone as shown in Figure 18, a distance of 2000 ft, the field measuring sites would be influenced somewhat by the diffraction of the field stress around the mining zone. The increase in vertical stress at these locations should be less than 30 per cent and, considering the amount of load carried by the pillars, should be only about 3 per cent.

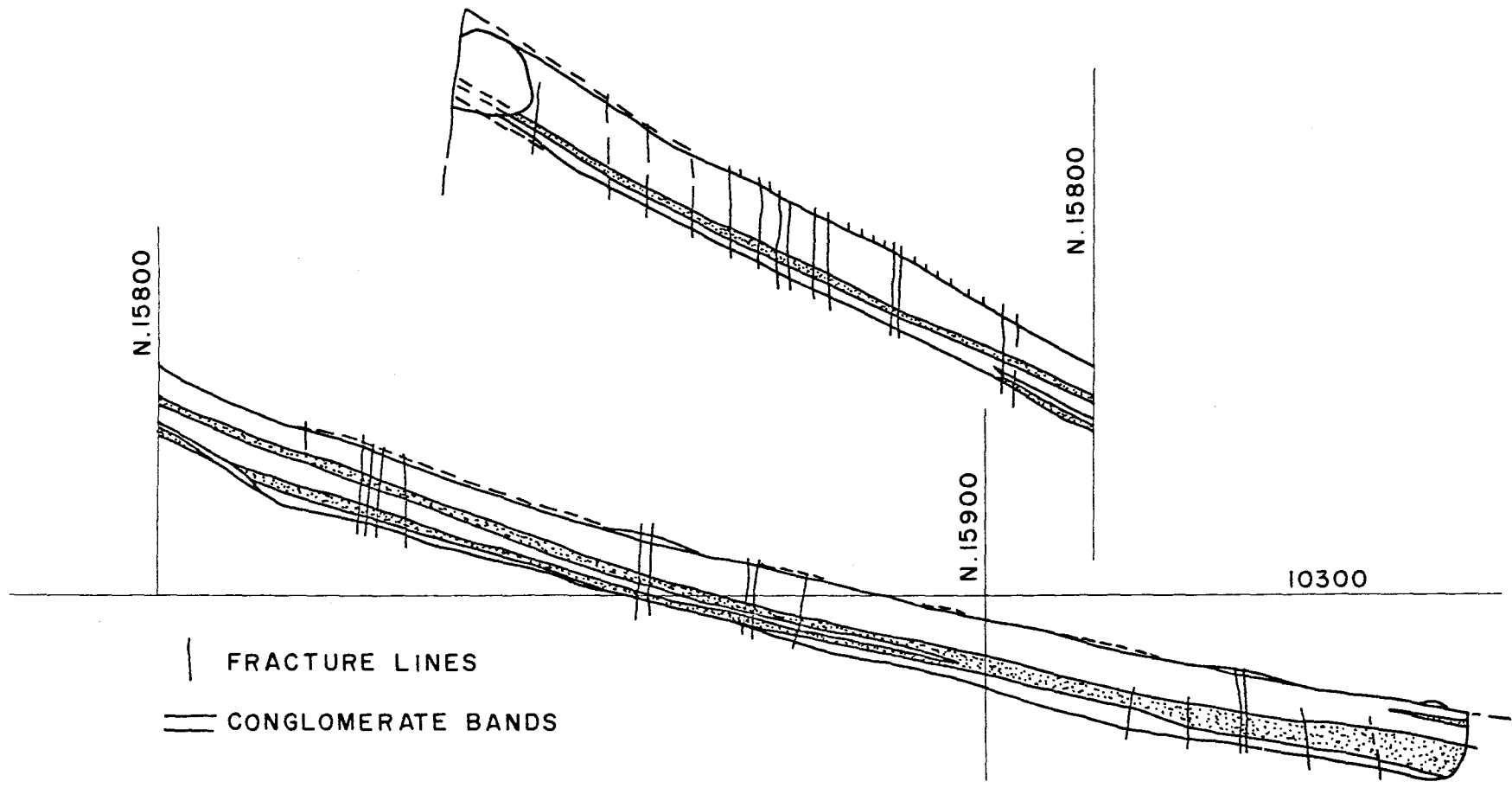


Figure 22. Section of west rib pillar, 9 W 9 stope (Ref. 12).

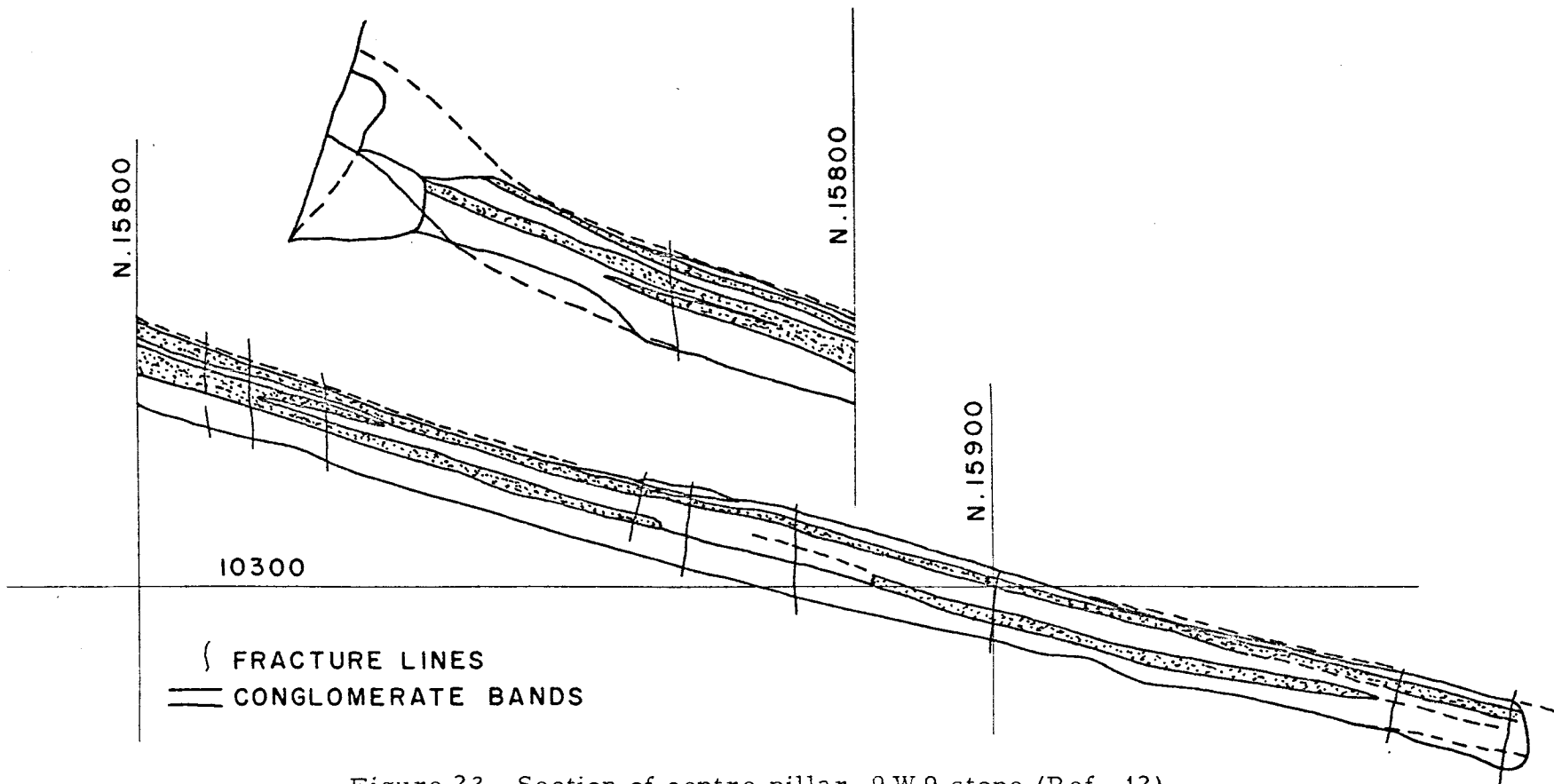


Figure 23. Section of centre pillar, 9 W 9 stope (Ref. 12).

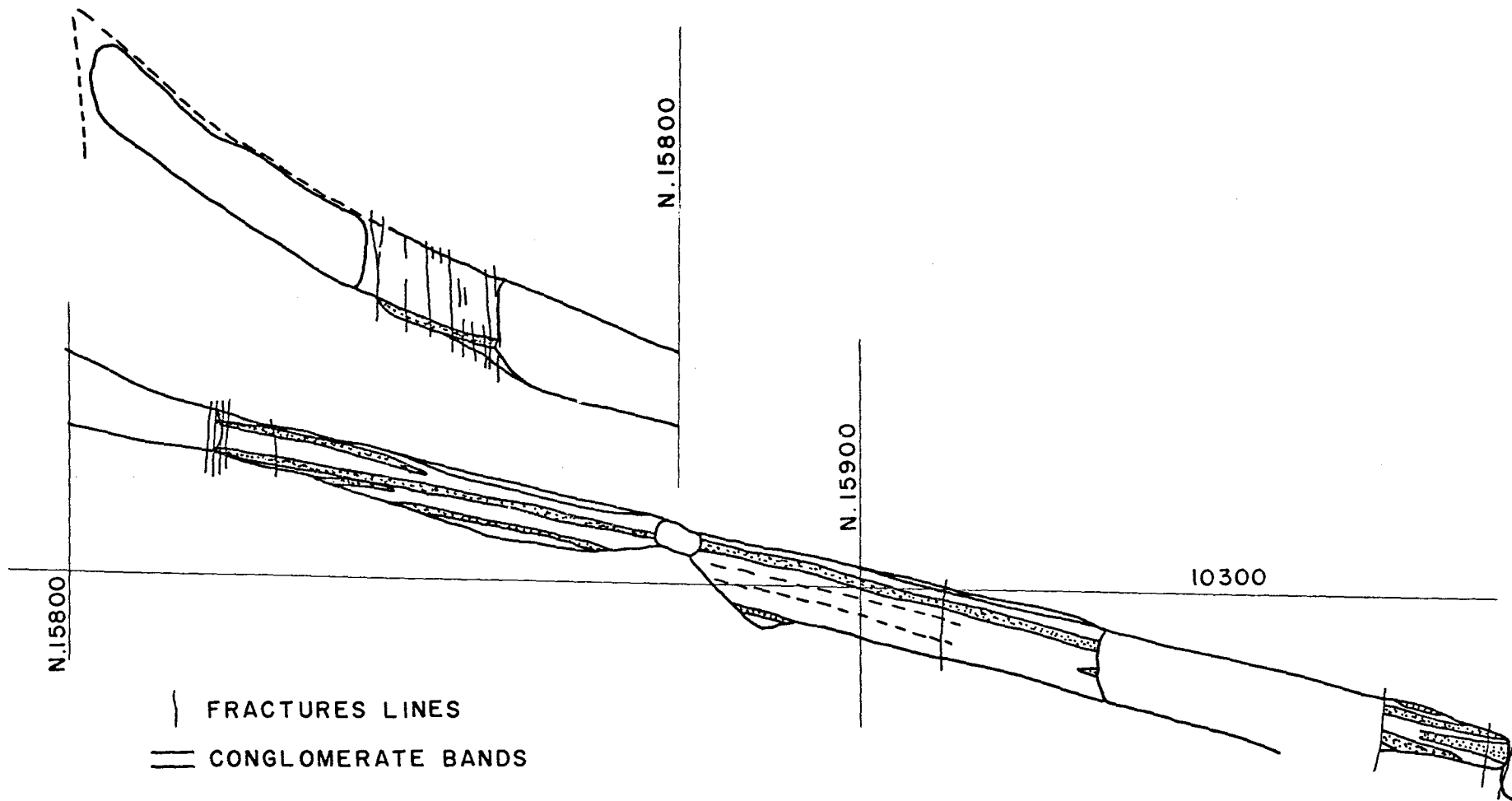


Figure 24. Section of east rib pillar, 9 W 9 stope (Ref. 12).

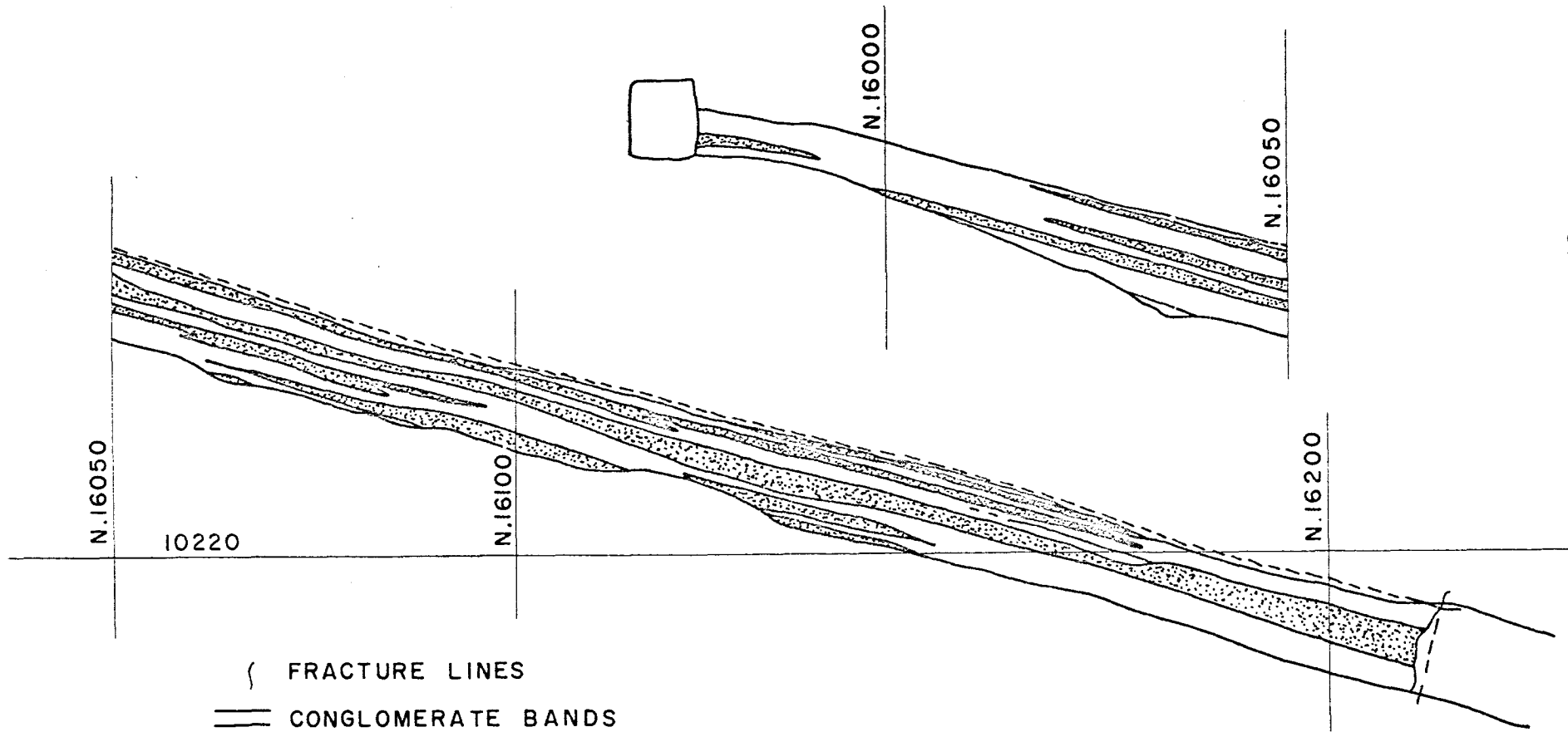


Figure 25. Section of west rib pillar, 1009 stope (Ref. 12).

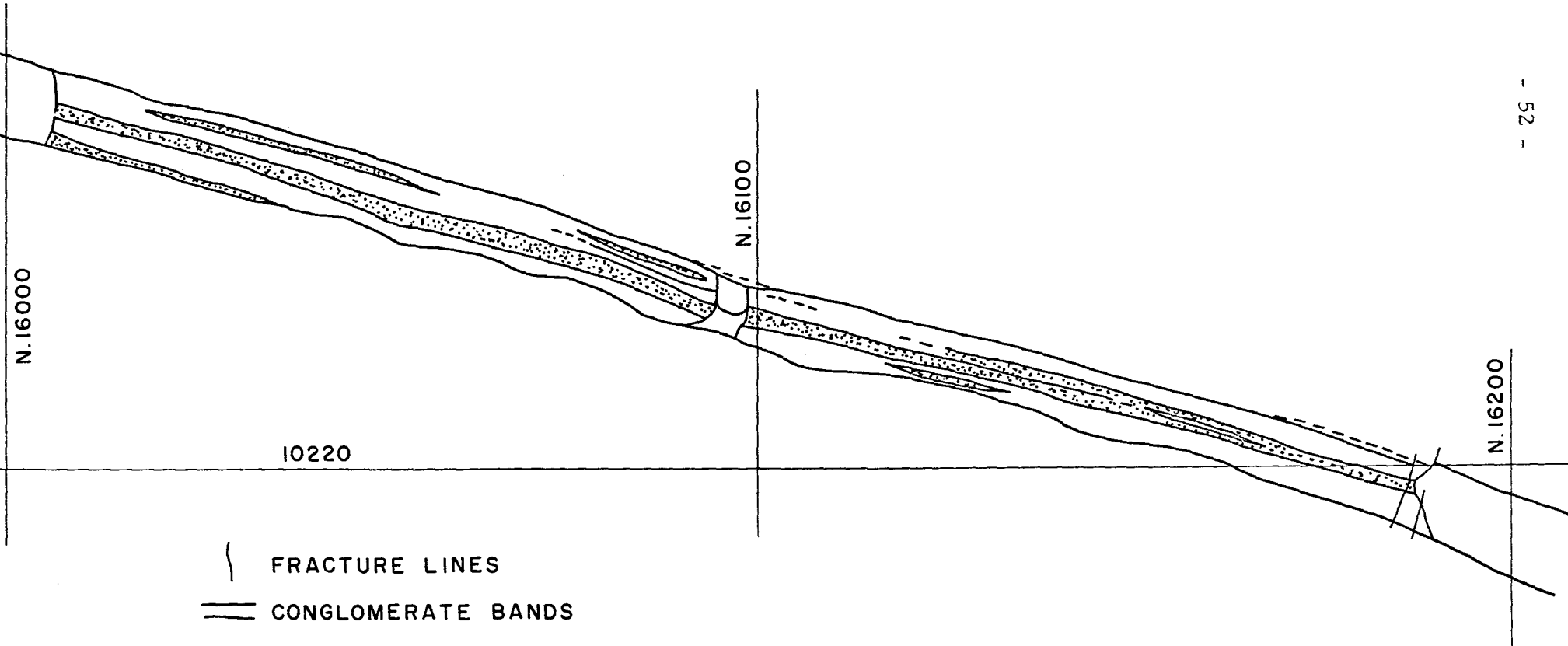


Figure 26. Section of centre pillar, 1009 stope (Ref. 12).

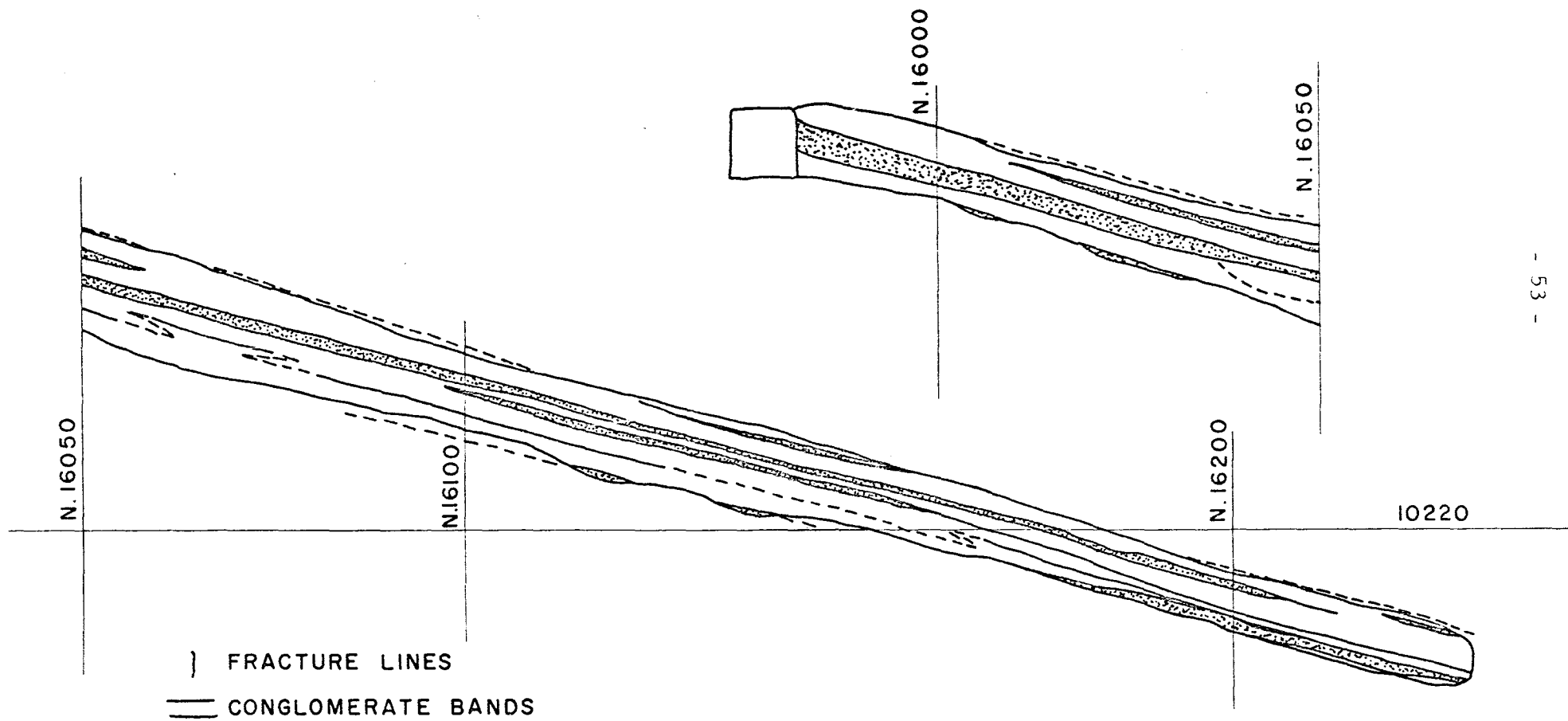


Figure 27. Section of east rib pillar, 1009 stope (Ref. 12).

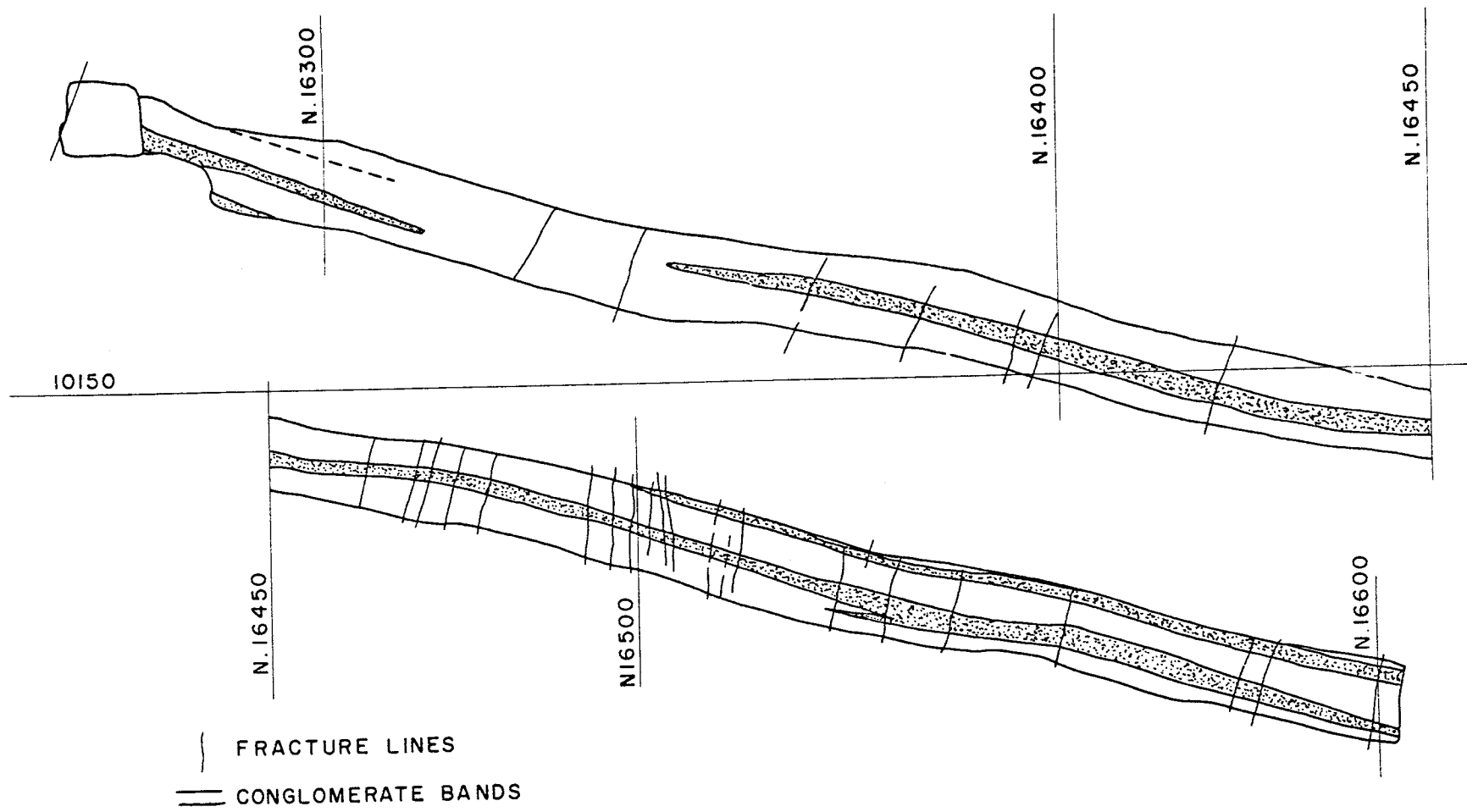


Figure 28. Section of west rib pillar, 1109 stope (Ref. 12).

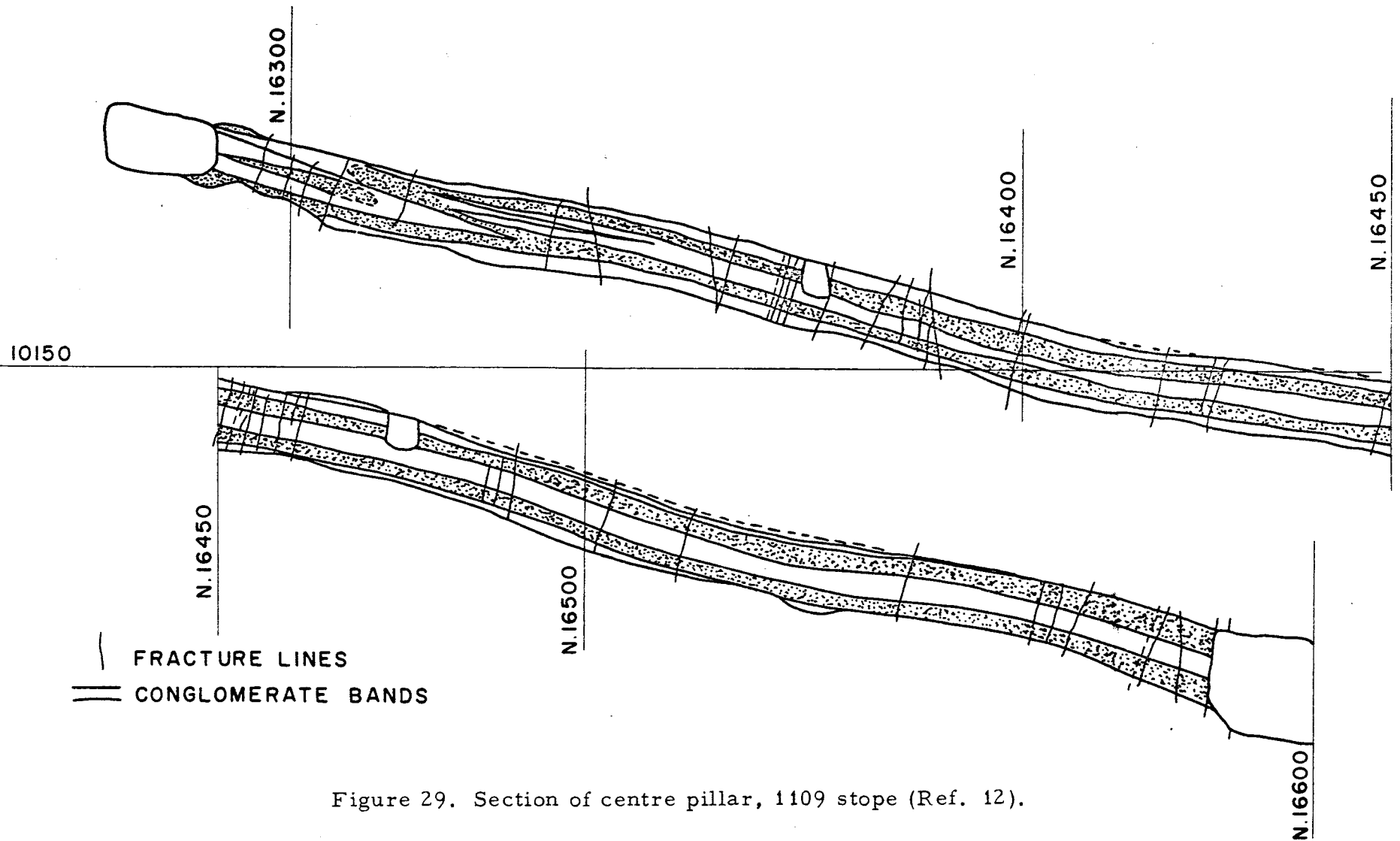


Figure 29. Section of centre pillar, 1109 stope (Ref. 12).

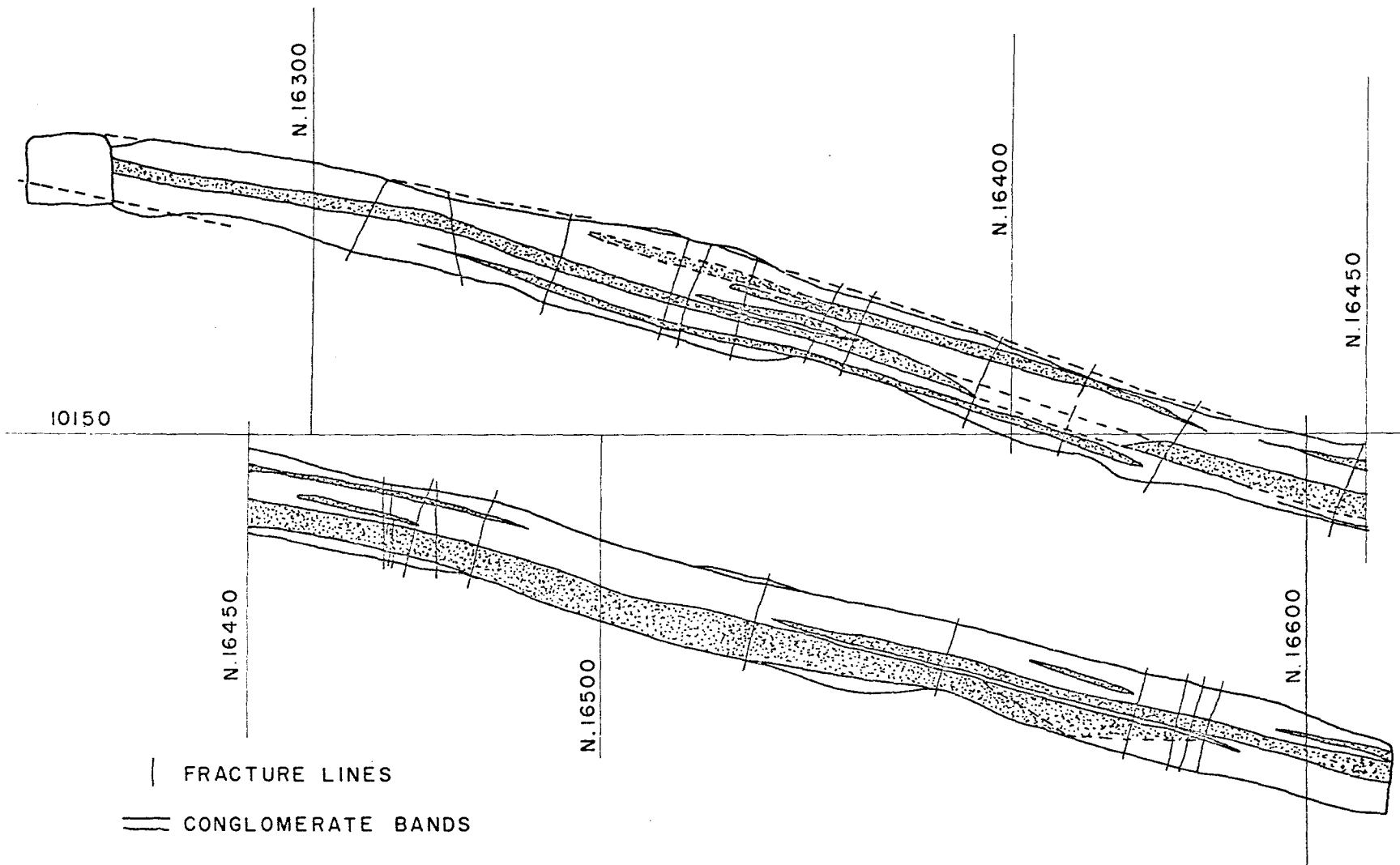


Figure 30. Section of east rib pillar, 1109 stope (Ref. 12).

There is also the possibility that the field stress is not homogeneous and was before mining somewhat different in the stoping area than in the present abutment zone. Without measurements having been taken before mining started and with only a limited number of drifts or crosscuts for measurements out from the present mining zone, it is difficult to appraise this possibility.

From the field stress readings, the field stress parallel to the vein and transverse to the mining zone, S_t , is found to be approximately 3700 psi and the field stress normal to the vein, S_o , might be approximately 2500 psi. These stresses produce a parameter $k = 1.48$. On the other hand, the vertical stress at the 14 drift, being higher than the vertical stress due to gravity, might be a local effect due to past faulting. Consequently, it might be more appropriate to use the gravitational stress for the vertical field stress combined with the measured horizontal stress for the determination of S_o . This would give an average figure of $S_o = 1100$ psi and $k = 3.36$.

Analysis of Data. In Table 11 the first analysis of the data is presented. In this case, all the arbitrary factors are selected to produce the low end of the possible range of measured to calculated values. The span, L_1 , is assumed to be 900 ft; the normal stress, S_o , is assumed to be 1100 psi; and the analysis for a deep mining zone is used.

It can be seen here that the tributary area theory would predict an increase in pillar stress of 5.25 times the normal field stress, S_o . Applying this factor to the gravitational stress, the predicted increase in pillar stresses would vary from 5170 psi to 6140 psi; however, this ignores the effect of the dip of the vein, which is not taken into account in the tributary area theory.

The hypothesis would predict increases in pillar stresses varying from 4.4 to 5.3 S_o . If these factors were applied to the assumed normal field stress of 1100 psi, the predicted increase in pillar stresses would be from 4800 psi to 5800 psi. The measured increase in pillar stresses over the field stress of 1100 psi varied from 4400 psi to 12,600 psi.

The differences between measured and calculated stresses are large for this first set of assumptions. Also, the variations in measured pillar stresses do not correspond to the predicted variations. The effect of variation in the breadth of pillars should be slight, because the average breadth of the pillars and the average breadth of the stopes remained essentially constant, which means that the deflection of the walls at any particular point would be governed by these average figures rather than by minor local variations. However, the variation with the parameter x should be effective but may be obscured by the wide variation in measured values arising from other factors.

TABLE 11

First Analysis of Data from Uranium Mine

$R = 0.84 = r, h_1 = 0.011, k = 3.36, \mu = 0.16 = \mu_p, n = 1$

No.	b_1	x_1	$\Delta\sigma'_p$	$\Delta\sigma'_p$	$\Delta\sigma'_p$
			MEAS	TA	HYP
9-2R	0.009	0.76	6.4	5.25	4.6
9-3R	0.009	0.89	8.4	5.25	4.4
9-1L	0.016	0.62	6.0	5.25	4.7
9-2L	0.010	0.76	5.9	5.25	4.6
9-3L	0.012	0.89	11.5	5.25	4.4
9-1C	0.012	0.62	4.0	5.25	4.7
10-1R	0.011	0.09	5.6	5.25	5.3
10-2R	0.017	0.33	6.3	5.25	5.0
10-1L	0.016	0.09	5.2	5.25	5.3
10-2L	0.016	0.33	4.8	5.25	5.0
10-1C	0.010	0.09	10.0	5.25	5.3
10-2C	0.011	0.33	6.4	5.25	5.0
11-2R	0.015	0.44	8.5	5.25	4.9
11-1L	0.015	0.67	7.3	5.25	4.6
11-2L	0.012	0.44	8.6	5.25	4.9
11-1C	0.009	0.73	8.3	5.25	4.6
11-2C	0.012	0.53	7.5	5.25	4.8
11-3C	0.011	0.27	8.3	5.25	5.1

An examination of the measured increases in pillar stresses with distance downdip showed no discernible correlation. This would leave one to conclude that the depth, z , or the gravitation loading, was not relevant owing to the presence of residual vertical stresses greater than gravitational stresses.

It is possible that the variation in pillar stresses arises from variations in the parameter n , which in turn leads to variations in the effective parameter r . The interrelation of these two factors would lead to pillar stresses both lower and higher than those predicted by the above calculations for uniform conditions.

In addition, as the area obviously still reflects the effects of past crustal disturbances, it is conceivable that there may be local bands of residual stresses associated with faulting that are both greater than and less than the measured field stresses away from the mining zone. An examination of the individual borehole deformation readings with logs of the cores, and with local joint and stratigraphic patterns, showed no obvious connection between extreme values of the readings and these geological features. The only broad correlation that might exist is that 10 stope contained the fewest number of visible joints or faults and at the same time produced the lowest pillar stresses with the exception of those at 1C. The other two stopes contained a high frequency of joints which may have been associated with minor faulting (12).

Another possible pattern might be a diagonal band of high stress through 9 stope from 1R to 2C to 3L, all of which either disced or fractured after overcoring. A similar band might exist in 11 stope, where 1R and 3C produced discing as did the adjacent overcoring hole 10-1C.

Another interesting feature observed was that in the overcoring holes the amount of surface rock that was fractured and possibly not carrying the full pillar stress varied between 4 in. and 9 in.; at this stage in the subject, one would be inclined to expect a deeper zone of fractured or relaxed ground.

Table 12 contains the second analysis of the data. In this case, all the arbitrary factors are selected to produce the highest values of the ratio of measured-to-calculated pillar stresses. The span, L_2 , is assumed to be 2000 ft; the normal stress, S_0 , is assumed to be 2500 psi; and the analysis for a shallow mining zone is used.

With these assumptions the hypothesis would predict increases in pillar stresses varying from 5.7 to 6.6 S_0 . Multiplying these factors by the assumed normal field stress of 2500 psi, the predicted increases in pillar stresses are from 14,300 psi to 16,500 psi. The measured increases in pillar stresses over the field stress of 2500 psi varied from 3000 to 11,200 psi.

TABLE 12

Second Analysis of Data from Uranium Mine

$R = 0.84 = r$, $h_2 = 0.005$, $k = 1.48$, $\mu = 0.16 = \mu_p$, $n = 1$

No.	b_2	x_2	$\Delta\sigma'_p$	$\Delta\sigma'_p$
			MEAS	HYP
9-2R	0.004	0.2	2.3	6.4
9-3R	0.004	0.15	3.1	6.6
9-1L	0.007	0.27	2.1	6.3
9-2L	0.004	0.21	2.1	6.4
9-3L	0.005	0.15	4.5	6.6
9-1C	0.005	0.27	1.2	6.3
10-1R	0.005	0.51	1.9	6.1
10-2R	0.008	0.40	2.2	6.2
10-1L	0.007	0.51	1.7	6.1
10-2L	0.007	0.40	1.5	6.2
10-1C	0.004	0.51	3.9	6.1
10-2C	0.005	0.40	2.3	6.2
11-2R	0.007	0.75	3.0	5.9
11-1L	0.007	0.85	2.7	5.7
11-2L	0.005	0.75	3.2	5.9
11-1C	0.004	0.88	3.1	5.7
11-2C	0.006	0.79	2.7	5.8
11-3C	0.005	0.67	3.1	6.0

The differences between measured and calculated stresses are also large for this second set of assumptions. Whereas in the first case the predicted stresses were lower than the measured stresses, in the second analysis the predicted stresses are higher than the measured stresses.

The discrepancy between predicted and measured pillar stresses could probably be reduced by improvements in field measurements. For example, if measurements of the field stress had been made in the actual mining zone before mining occurred, it is possible that different values would have been obtained than those measured in the present abutment zone. If the field stress normal to the vein, S_0 , had an intermediate value between the two extremes assumed in the above calculations, the agreement between the calculated and average field values would be very close. The dispersion in measured values would remain, but these could probably be predicted either by having measured the variations in the field stresses or by having measured variations in the compressibility of the pillars.

CONCLUSIONS

The main conclusion to be drawn from the field studies is that the field stresses around a mine cannot be assumed to be homogeneous. In addition, it is becoming clear that horizontal field stresses are quite commonly greater than vertical field stresses. For additional pillar studies, more field work should be conducted on the determination of relative compressibility, or the parameter n , of pillar rock, which seems to be one of the most influential parameters in actual mines.

The tributary area theory was found not to predict actual pillar loadings with acceptable accuracy nor to account for changes in pillar loadings resulting from changes in such parameters as x , z/L , N , h , b , k and n .

With a hypothesis for predicting pillar loading, it appears that at least the practical objective of being able to predict the consequences of mining at lower levels in the same rock might be obtainable. For example, a situation could arise in which when mining at a depth of 500 ft with an extraction ratio of 85 per cent no failure occurred, whereas when mining at a depth of 1000 ft with an extraction ratio of 80 per cent minor slabbing was produced. The question could then be asked: "What would be the appropriate extraction ratio or breadth of pillars for mining the same ore at a depth of 2000 ft?" Using the hypothesis, it would be possible to predict,

with the degree of accuracy depending on the constancy of other parameters, the appropriate mine geometry for complete stability as occurred at a depth of 500 ft or for minor instability as occurred at 1000 ft. In other words, using the hypothesis it should be possible to predict, other things being equal, the effects of increased depths, the effects of any change in field stress, pillar height, pillar breadth and pillar compressibility.

ACKNOWLEDGEMENTS

The new field data included in this report were obtained through the valuable work of F. Grant, I. Bain, Y. Yu, A. St. Louis, W. Zawadski and J. St. Onge. Miss M. Ellis provided valuable assistance in compiling the manuscript, and the editing was done with the good services of Mr. P.E. Shannon. Mr. E.R. Leeman of the C.S.I.R. in South Africa provided helpful supplementary information.

- - - -

DFC:DV

BIBLIOGRAPHY

1. Coates, D.F., "Pillar Loading. Part I: Literature Survey and New Hypothesis", Mines Branch Research Report R 168, Department of Mines and Technical Surveys, Ottawa, Canada (Oct. 1965).
2. Coates, D.F., "Pillar Loading. Part II: Model Studies", Mines Branch Research Report R 170, Department of Mines and Technical Surveys, Ottawa, Canada (Nov. 1965).
3. Duvall, W., "Stress Analysis Applied to Underground Mining Problems. Part II: Stress Analysis Applied to Multiple Openings and Pillars", USBM RI4387 (1948).
4. Hast, N., "The Measurement of Rock Pressure in Mines", Sveriges Geologiska Undersokning, Arsbok 52, No. 3, Stockholm (1958).
5. Geldart, L. and Udd, J., "Boundary Stresses Around an Elliptical Opening in an Infinite Solid", Proc. Rock. Mech. Symp., McGill Univ., Mines Branch (1963).
6. Leeman, E.R. and van Heerden, W., "Stress Measurements in Coal Pillars", Colliery Engineering (Jan. 1964).
7. Canadian Mining Journal, Vol. 77, No. 11 (1956).
8. Merrill, R. et al., "Stress Determinations by Flatjack and Borehole-Deformation Methods", USBM RI6400 (1964).
9. Merrill, R. and Peterson, J., "Deformation of a Borehole in Rock", USBM RI 5881 (1961).
10. Coates, D.F. and Grant, F., unpublished reports (1965).
11. Morrison, R.G.K., Corlett, A. and Rice, H.R., "Report of the Special Committee on Mining Practices at Elliot Lake", Bull. 155, Ontario Dept. of Mines (1961).
12. Bain, I., unpublished report (1965).

APPENDIX

GLOSSARY OF ABBREVIATIONS

Note: After many of the terms, letters in brackets indicate the fundamental dimensions of the physical quantity; e. g., L stands for length, M for mass, F for force, T for time, and S signifies that the quantity is dimensionless.)

$a(L)$	- radius of a circle or major semi-axis of an ellipse
$A_o(L^2)$	- total area of walls adjacent to the mined-out rooms or stopes of the entire mining zone
$A_p(L^2)$	- area of a pillar parallel to the walls
$A_t(L^2)$	- area of walls tributary to a pillar
$A_T(L^2)$	- area of walls adjacent to the entire mining zone
$b(D)$	- width of pillar (B/L)
$b(L)$	- minor semi-axis of an ellipse
$b_o(D)$	- width of opening (B_o/L)
$B(L)$	- width of pillar
$B_o(L)$	- width of opening (stope or room)
$cc(L)$	- centre to centre
$cc(L^3)$	- cubic centimetre
$cf(L^3)$	- cubic foot
$c(FL^{-2})$	- cohesion
$ci(L^3)$	- cubic inch
$cm(L)$	- centimetre
cpn	- compression
$C_b(D)$	- coefficient of $\frac{WL^3}{EI}$ for calculating the deflection of a beam due to bending moment
$C_s(D)$	- coefficient of $\frac{WL^3}{EI}$ for calculating the deflection of a beam due to shear force
$d(D)$	- parameter of an ellipse ($3 - 4\mu$) in plane strain and $(3 - \mu)/(1 + \mu)$ in plane stress
$dia(L)$	- diameter

Eq.	- equation
$E(FL^{-2})$	- modulus of linear deformation (Young's modulus)
$E_p(FL^{-2})$	- modulus of deformation of pillar rock
ft(L)	- feet
$F_s(D)$	- factor of safety
$G(FL^{-2})$	- modulus of shear deformation
$h'(L)$	- semi-height of a pillar
$h(D)$	- dimensionless height of a pillar (H/L)
$H(L)$	- height of pillar
$i(D)$	- angle of dip to horizontal
in. (L)	- inch
$I(L^4 \text{ or } ML^2)$	- moment of inertia
$k(D)$	- S_t/S_o or σ_h/σ_v
$k_s(L^3F^{-1})$	- coefficient of subgrade reaction, δ/q
ksc	- kilograms per square centimetre
l	- semi-span of a mining zone ($L/2$)
$\ln a$	- natural logarithm of a
$\log a$	- logarithm of a to base 10
LF	- linear foot
$L(L)$	- breadth of mining zone
max	- maximum
$m(D)$	- Poisson's number
$m(D)$	- parameter of an ellipse $(a-b)/(a+b)$
min	- minimum

$M (FL^{-2})$	- $E/(1 - \mu^2)$
$M (FL)$	- moment
$n (D)$	- ratio of moduli of deformation (M/M_p or E/E_p)
$N (D)$	- number of pillars
$p (FL^{-2})$	- contact pressure
$pcf (FL^{-3})$	- pounds per cubic foot
$psf (FL^{-2})$	- pounds per square foot
$psi (FL^{-2})$	- pounds per square inch
$P (F)$	- a pillar load
$q (FL^{-2})$	- bearing pressure
$Q_B (FL^{-2})$	- uniaxial compressive strength of a sample of width B
$Q_o (FL^{-2})$	- uniaxial compressive strength for a sample of unit width
$Q_u (FL^{-2})$	- uniaxial compressive strength
$r (D)$	- local extraction ratio, i. e. based on tributary area to single pillar
$r (L)$	- radius or radial distance
$R (D)$	- extraction ratio (wall area excavated/total wall area); parameter of an ellipse $(a + b)/2$
$R (L)$	- radius or radial distance
$sf (L^2)$	- square foot
$si (L^2)$	- square inch
$S (L^{-3})$	- section modulus
$S_h (FL^{-2})$	- field stress in the horizontal direction

$S_t (FL^{-2})$	- field stress parallel to the seam or vein and normal to strike
$S_v (FL^{-2})$	- field stress in the vertical direction
$S_o (FL^{-2})$	- field stress normal to seam or vein
$S_p (FL^{-2})$	- average pillar pressure on walls $\Sigma P / \Sigma A_t$
$S_x (FL^{-2})$	- field stress in the x-direction
$S_y (FL^{-2})$	- field stress in the y-direction
$S_z (FL^{-2})$	- field stress in the z-direction
tsn	- tension
TA	- tributary area
$v_r (L)$	- radial displacement
$v_\theta (L)$	- tangential displacement
V(F)	- shear force
w (D)	- $\mu / (1 - \mu)$
wrt	- with respect to
$W (F \text{ or } MLT^{-2})$	- load or weight
x (L or D)	- linear displacement or co-ordinate or dimensionless distance (x'/L) in direction of x-axis
$x' (L)$	- linear displacement or co-ordinate in direction of x-axis
y (L)	- linear displacement or co-ordinate in direction of y-axis
$z' (L)$	- dimensionless co-ordinate (z/L) in direction of z-axis
z (L or D)	- linear displacement or co-ordinate in direction of z-axis

- $\delta(L)$ - inward displacement of wall normal to vein or seam; or just displacement
- $\delta'(L)$ - reverse displacement of wall due to average pillar pressure
- $\delta A(L)$ - abutment compression or deformation
- $\delta_c(L)$ - displacement of wall normal to vein or seam at centreline
- $\delta_e(L)$ - inward displacement of wall normal to vein (or seam), resulting from excavation of stopes or rooms
- $\delta'_p(L)$ - local penetration of a pillar into the wall
- $\delta_x(L)$ - displacement of wall normal to vein or seam at x from centreline
- $\gamma(D)$ - shear strain
- $\gamma(\text{FL}^{-3})$ - unit weight (bulk density)
- $\epsilon(D)$ - linear strain
- $\epsilon_r(D)$ - linear strain in the radial direction
- $\epsilon_t(D)$ - linear strain in the tangential direction
- $\epsilon_\theta(D)$ - linear strain in the tangential direction
- $\mu(D)$ - Poisson's ratio
- $\rho(L)$ - radius of curvature
- $\sigma(\text{FL}^{-2})$ - normal stress
- $\sigma_p(\text{FL}^{-2})$ - pillar stress P/A_p
- $\bar{\sigma}_p(D)$ - σ_p/S_o
- $\sigma_p(\text{FL}^{-2})$ - average pillar stress $\Sigma P/\Sigma A_p$
- $\Delta\sigma_p(\text{FL}^{-2})$ - increase in pillar stress due to mining

$\Delta\sigma_p'(D)$	- $\Delta\sigma_p/S_o$
$\sigma_r(FL^{-2})$	- radial stress
$\sigma_\theta(FL^{-2})$	- tangential stress
$\sigma_t(FL^{-2})$	- tangential stress
$\sigma_1(FL^{-2})$	- major principal stress
$\sigma_2(FL^{-2})$	- intermediate principal stress
$\sigma_3(FL^{-2})$	- minor principal stress
$\tau(FL^{-2})$	- shear stress

CONVERSION TABLES - BRITISH, AMERICAN AND METRIC UNITS OF MEASUREMENT

To convert	Into	Multiply by:
L E N G T H		
inches	centimetres	2.54
feet	metres	0.3048
yards	metres	0.9144
miles (statute)	kilometres	1.609344
centimetres	inches	0.3937
metres	feet	3.281
kilometres	miles (stat.)	0.6214
microns	metres	1 x 10 ⁻⁶
A R E A		
square inches	square centimetres	6.4516
	square feet	0.006944
square feet	square centimetres	929.03
square yards	square metres	0.8361
square miles	square kilometres	2.590
square centimetres	square inches	0.1550
square metres	square feet	10.76
square kilometres	square miles	0.3861
V O L U M E		
cubic inches	cubic centimetres	16.39
cubic feet	cubic metres	0.02832
cubic metres	cubic inches	61023
	cubic feet	35.31
D E N S I T Y		
pounds/cubic foot	kilograms/cu.metre	16.02
kilograms/cu.metre	pounds/cubic foot	0.06243
M A S S		
pound (English)	gram	453.6
gram	pound	2.205 x 10 ⁻³
Slug (American)	kilogram	14.59
	pound	32.17

To convert	Into	Multiply by:
V E L O C I T Y		
inches/second	centimetres/second	2.54
feet/second (fs)	centimetres/second	30.48
miles/hour	centimetres/second	44.70
	kilometers/hour	1.609
centimetres/second	feet/second	0.03281
	miles/hour	0.02237
kilometres/hour	feet/second	0.9113
	miles/hour	0.6214
A C C E L E R A T I O N		
inches/second ²	centimetres/second ²	2.54
	g	0.0029
feet/second ²	centimetres/second ²	30.48
	g	0.0311
centimetres/second ²	inches/second ²	0.3937
	feet/second ²	0.03281
g	centimetres/second ²	980.6
	feet/second ²	32.17
F O R C E		
pounds (American)	dynes	44.482 x 10 ⁴
	grams	453.6
dynes	pounds	2.248 x 10 ⁻⁶
	grams	1.02 x 10 ⁻³
grams	pounds	2.205 x 10 ⁻³
	dynes	980.7
poundals	dynes	13,826
	pounds	0.03108
newtons	dynes	1 x 10 ⁵
P R E S S U R E & S T R E S S		
pounds/square inch	kilogram/centimetre ²	0.0703
pounds/square foot	kilogram/metre ²	4.882
kilogram/centimetre ²	pounds/square inch	14.22
	pounds/square foot	2048
bars	dynes/centimetre ²	10 ⁶
	kilograms/metre ²	1.020 x 10 ⁴
	pounds/squre inch	14.50
	pounds/square foot	2089